AD NUMBER
AD513612
CLASSIFICATION CHANGES
TO: **UNCLASSIFIED**
FROM: **CONFIDENTIAL**
LIMITATION CHANGES
TO: **Approved for public release; distribution is unlimited.**
FROM: **Distribution authorized to U.S. Gov't. agencies only; Administrative/Operational Use; JAN 1971. Other requests shall be referred to Air Force Avionics Lab., Wright-Patterson AFB, OH 45433.**
AUTHORITY
AFAL ltr 12 Jan 1976 ; AFAL ltr 12 Jan 1976

SECURITY MARKING

The classified or limited status of this report applies to each page, unless otherwise marked.
Separate page printouts MUST be marked accordingly.

THIS DOCUMENT CONTAINS INFORMATION AFFECTING THE NATIONAL DEFENSE OF THE UNITED STATES WITHIN THE MEANING OF THE ESPIONAGE LAWS, TITLE 18, U.S.C., SECTIONS 793 AND 794. THE TRANSMISSION OR THE REVELATION OF ITS CONTENTS IN ANY MANNER TO AN UNAUTHORIZED PERSON IS PROHIBITED BY LAW.

NOTICE: When government or other drawings, specifications or other data are used for any purpose other than in connection with a definitely related government procurement operation, the U. S. Government thereby incurs no responsibility, nor any obligation whatsoever; and the fact that the Government may have formulated, furnished, or in any way supplied the said drawings, specifications, or other data is not to be regarded by implication or otherwise as in any manner licensing the holder or any other person or corporation, or conveying any rights or permission to manufacture, use or sell any patented invention that may in any way be related thereto.

AFAL-TR-70-280

(UNCLASSIFIED TITLE)

NUTATRON GYRO DEVELOPMENT

Edward J. Harrison, et al.
Bell Aerospace Company

TECHNICAL REPORT AFAL-TR-70-280

JANUARY 1971

DOWNGRADED AT 3 YEAR INTERVALS
DECLASSIFIED AFTER 12 YEARS
DOD DIR 5200. 10

Air Force Avionics Laboratory (AVNE)
Air Force Systems Command
Wright-Patterson Air Force Base, Ohio 45433

STATEMENT #3 CLASSIFIED

In addition to security requirements which apply to this document and must be met, each transmittal outside the agencies of the U.S. Government must have prior approval of _____

NOTICE

When Government drawings, specifications, or other data are used for any purpose other than in connection with a definitely related Government procurement operation, the United States Government thereby incurs no responsibility nor any obligation whatsoever; and the fact that the government may have formulated, furnished, or in any way supplied the said drawings, specifications, or other data, is not to be regarded by implication or otherwise as in any manner licensing the holder or any other person or corporation, or conveying any rights or permission to manufacture, use, or sell any patented invention that may in any way be related thereto.

Copies of this report should not be returned unless return is required by security considerations, contractual obligations, or notice on a specific document.

AFAL-TR-70-280

(UNCLASSIFIED TITLE)

NUTATRON GYRO DEVELOPMENT

Edward J. Harrison, et al.

FOREWORD

(UNCLASSIFIED FOREWORD)

This final technical report on a bearing study phase of the Nutatron development was prepared by Bell Aerospace Company in accordance with the requirements of Air Force Contract F33615-69-C-1722. The program was accomplished under the direction of the Air Force Avionics Laboratory. Mr. Robert McAdory (AFAL/NVE) was Project Engineer for the laboratory. This phase of the program was sponsored by the Air Force and began April 1, 1969 and was completed September 1, 1970. The program was carried out at Bell Aerospace Company, P.O. Box 1, Buffalo, New York, in the Inertial Instrument Section; Ernest H. Metzger, Chief Engineer. The following lead personnel of this section contributed to the program:

Mr. Edward J. Harrison, Program Manager
Dr. Don R. Allen, Theoretical Analysis and Investigation
Mr. Giles M. Hofmeyer, Test and Evaluation
Mr. F. D. McCollum, Mechanical Design
Mr. Robert F. Martin, Bearing Analysis and Investigation

This report was submitted September 1970.

This report contains no classified information extracted from other classified documents.

This technical report has been reviewed and is approved.

WILLIAM J. DELANEY
Lt Colonel, USAF
Chief, Navigation & Guidance Division

ABSTRACT

(UNCLASSIFIED ABSTRACT)

This phase of the Nutatron gyroscopic sensor development was sponsored by the Air Force Avionics Laboratory, WPAFB under Contract F33615-69-C-1722 and by Bell Aerospace Company. The Nutatron gyro features an anisometric rotor which responds to torques by exhibiting minute signals at twice the rotor frequency. These signals are used to automatically compensate for the drift producing torques and as a result the Nutatron is a high performance, low cost gyro with fast reaction time. Under previous contracts, the feasibility of the concept was demonstrated and an engineering model was designed, fabricated, and tested. This report covers a phase of the instrument development which had as its goal the investigation of the effect of bearing imperfections on the instrument performance. During this program unique analyses of bearing noise were made and the results of these analyses show which bearing parameters are important to achieving good Nutatron performance.

CONTENTS

ILLUSTRATIONS

TABLES

SYMBOLS USED IN SECTION III-C

F_a = Axial Load
F_r = Radial Load
Q_ψ = Individual Ball Load
α = Loaded Contact Angle
ψ = Ball Position Angle
δ_a = Axial displacement
δ_r = Radial displacement
K_n = Ball load vs. ball race deformation coefficient
A = $r_o + r_i - D$
r_o = Radius of curvature of outer race
r_i = Radius of curvature of inner race
$\overline{\delta}_a$ = δ_a/A normalized axial displacement
$\overline{\delta}_r$ = δ_r/A normalized radial displacement
δ_n = The normal approach of the races
$\overline{\theta}$ = θ/A normalized angular displacement
α° = free contact angle
R_i = Radius of locus of centers of curvature of inner race.
R_o = Radius of locus of centers of curvature of outer race.

SYMBOLS FOR APPENDIX B

a = ridge width
a_l = groove width
h = ridge clearance normal to surfaces
h_l = groove clearance normal to surfaces
k_a = axial spring constant
k_r = radial spring constant
r = radius
r_i = small conical radius
r_o = large conical radius
x = direction of motion of model slider
y = direction perpendicular to motion of model slider
F = force
F_a = axial force
F_r = radial force
P = ridge pressure
P_l = groove pressure
P_o = average pressure at y, ϕ
U = slider linear speed
α = cone angle
γ = groove depth to clearance ratio (Δ/h)
δ = bearing deflection normal to surface
ϵ = ratio of bearing deflection to clearance (δ/h)
ξ = coordinate perpendicular to groove
η = coordinate along groove
θ = groove angle
μ = lubricant viscosity
ρ = lubricant density
σ_a = axial deflection
σ_r = radial deflection
ϕ = circumferential conical coordinate
ω = angular speed
Δ = groove depth
$[\,]_S$ = quantity pertaining to seal belt
$[\,]_G$ = quantity pertaining to grooved area

SECTION I

INTRODUCTION

This document constitutes the final report on a unique bearing study phase of the Nutatron development program. Initially this phase was to cover the design and incorporation of a hydrodynamic gas bearing in the Nutatron gyro engineering model. Due to a change in the funding situation, the work statement was revised to cover the design of a gas bearing and a noise analysis of the Nutatron ball bearing. The Air Force Avionics Laboratory, sponsored this program under Contract No. F33615-69-C-1722.

The Nutatron is an angular rate sensor using an anisometric rotor. The instrument responds to gyroscopic torques by exhibiting minute oscillations at twice the rotor frequency in addition to conventional gyro drift. An automatic feedback loop senses these minute oscillations and nulls the drift which produces them. Hence, continuous drift compensation is provided and the requirement to stabilize torques prior to a navigation mission is eliminated. As a result, the Nutatron is a high performance gyro with an extremely short readiness time (less than one minute).

During previous phases of the Nutatron development effort, a Nutatron engineering model was designed, fabricated and tested. Several error mechanisms were identified and corrected so that the only major remaining source of error is noise at twice the rotor frequency arising from the ball type spin bearings. Under this phase detailed examination of the characteristics of the bearing noise was undertaken. The steps required to reduce the effects of bearing noise are now known and can be incorporated in the instrument in a subsequent effort. Table I illustrates the effect these steps will have. When these steps have been taken, the instrument will be ready for an independent evaluation program at a facility such as Holloman AFB.

The body of this report is devoted to the work completed under this phase of the development only. A discussion of the Nutatron theory and a description of the engineering model can be found in Technical Reports AFAL-TR-65-170, AFAL-TR-67-54, and AFAL-TR-69-76.

SECTION II

SUMMARY

The primary task of this program was a bearing study effort including the design of a low speed gas bearing for the Nutatron and a thorough analysis, supplemented by a test effort, of ball bearing noise specifically at the Nutatron frequency. The results of these efforts showed that:

1. The spin bearings are the major remaining source of error producing noise. This noise affects performance in four ways;

a) Geometric errors in the bearing produce noise at twice the rotor frequency. However, this source has been shown to be very small.

b) Improper mounting of the bearing is the major source of noise that is g sensitive. This can be corrected with minor modification to the rotor structure.

c) Bearing noise occuring around the spin axis is cross coupled into the input axes by means of the flex leads. The use of very compliant flex leads will eliminate this problem.

d) Beating between the ball complement speeds of the two spin bearings gives rise to a low frequency "random" drift component. Purposely introducing a difference in the two bearings will raise the beat frequency so that it can be filtered.

2. When the modifications described above have been incorporated, the Nutatron will be ready for evaluation by an independent test facility.

3. A low speed gas bearing for the Nutatron is feasible. Although improved performance is anticipated, a thorough study of gas bearing noise at the Nutatron frequency should be undertaken before such a bearing is used.

SECTION III
TECHNICAL DISCUSSION

The approach being used in the development of the Nutatron gyro is one that combines investigative testing of an engineering model supported by a rigorous theoretical analysis of potential error mechanisms. When an error source is identified by this approach, appropriate changes are made to either the instrument or the electronics to eliminate the error source. Calibration and/or trimming to reduce the error level are avoided because these operations lead to expensive instruments and provide a source of potential failure if changes occur due to aging, temperature, etc.

A. Major Results of the Test/Analysis Effort

The results of the test/analysis effort show that four sources of error remain.

1. Noise at twice the rotor frequency due to imperfections in the bearing races. This error source is not a limiting factor at the present level of performance, but does represent an area of potential improvement. Analysis of the bearing errors show that a sufficient improvement can be obtained without the use of expensive specially made bearings. This improvement requires a change in the ball count and contact angle of the spin bearings.

2. Noise at the Nutatron frequency resulting from improper mounting of the bearing. This has been shown experimentally and analytically to be the largest source of g-sensitive noise. G-sensitive motion at twice per revolution results from unequal bearing compliances in the major axes of the rotor (see Figure 1).

Under radial acceleration, the bearing deflects along the acceleration vector by

$$d = \frac{Ma}{K}$$

where M = the rotor mass
a = acceleration
K = compliance of bearing

From this it can be seen that if $K_x \neq K_y$, the deflection of the bearing has a component at twice per revolution in addition to a steady-state value. Misalignment of the bearings results in unequal distribution of the preload. This in turn produces the unequal compliances around the bearing due to the inherent nonlinearity of the ball compliance. A more detailed analysis of the phenomena is given in Section III.C.

An improved method of mounting the bearings in the rotor structure will result in a significant reduction of this error source without increasing the complexity of the instrument.

3. Cross coupling of noise about the spin axis into the input axes by the flex leads. Both g-insensitive noise and random noise have been shown to arise from this source. The cross coupling effect has been traced to the fact that the flex leads do not lie in a plane through the center of

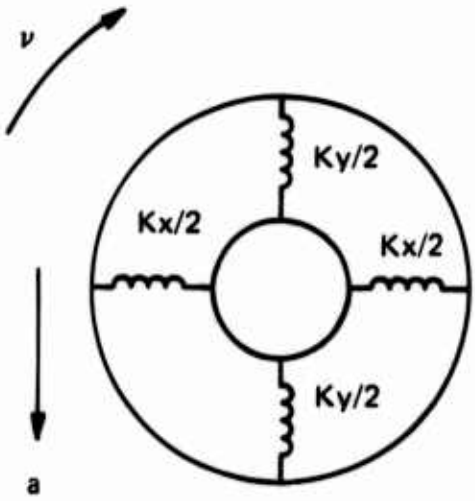

Figure 1. Unequal Bearing Compliance

suspension. As noise, $\theta_N \sin 2\nu t$, around the spin axis exercises the flex leads (Figure 2) a force is developed in each flex lead which is

$$f = K_F \theta_N \sin 2\nu t.$$

Because the plane of the flex leads is displaced from the center of suspension by the distance ℓ the flex lead forces are converted to a torques about an input axis.

$$T = \ell K_F \theta_N \sin 2\nu t$$

If the flex compliances (K_{F_1}, K_{F_2} and K_{F_3}) are equal, a torque balance condition exists. Unequal compliances however, upset this balance and a torque at twice per revolution (2ν) is introduced into the input axis producing unwanted noise.

Elimination of this error source will be obtained by modifying the flexure pivot to permit the use of very compliant flex leads. The present suspension system requires stiff flex leads to prevent low frequency spin axis resonance.

4. A beating between the ball component frequencies of the two spin bearings adds a low frequency periodicity to the Nutatron output. Intentionally making the bearings at each end of the rotor slightly different will increase the beat frequency so that it is easily filtered.

The subsequent sections of this report provide detailed discussions of the test program as well as the analytical effort.

B. Summary of the Test Program

During the period covered by the contract, a continuous investigative test program was conducted on the Nutatron engineering model. The major effort was devoted to examining the characteristics of the Nutatron noise. This was accomplished by a series of exploratory tests in conjunction with some modifications to the gyro rotor. The parameters tested for were g-insensitive drift, g-sensitive drift, randomness and the temperature coefficient of these drifts. The present level of performance of these parameters is illustrated by Table I. The significant results of the test program are discussed below.

1. Measurement of g-Sensitive Noise

Under normal circumstances, the g-sensitive Nutatron noise is measured by positioning the gyro spin axis parallel to the earth rotation axis. In this position approximately 0.7 g is introduced in the input axis, but the earth rotation rate is not sensed. The gyro is operated in the normal rate constrained mode of operation with the case rotating. The difference between the noise level measured in this position and the systematic noise measured with the spin axis vertical is the g-sensitive noise.

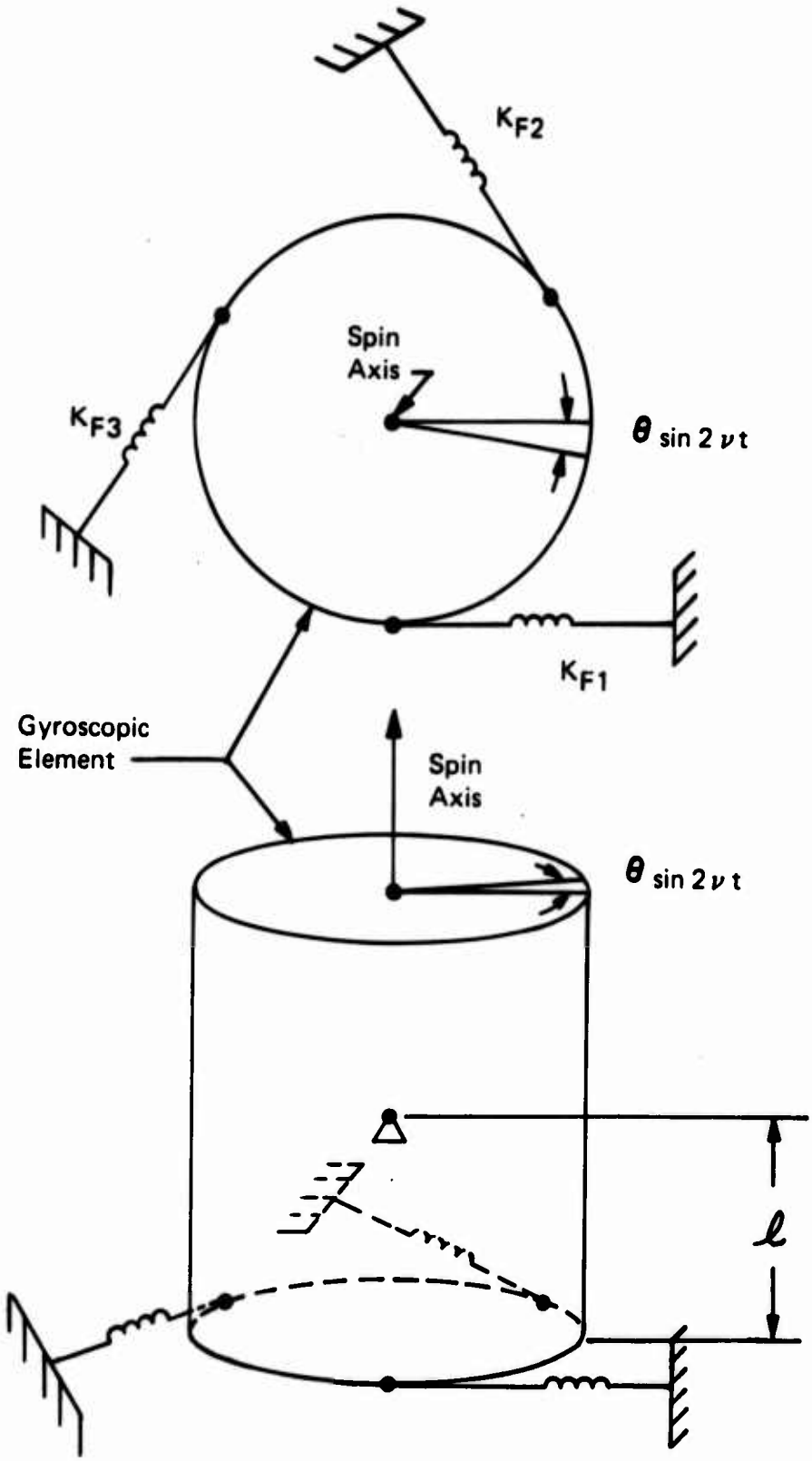

Figure 2. Flex Lead Cross Coupling

TABLE I
NUTATRON PERFORMANCE PARAMETERS

	Present	Anticipated
Systematic Drift Repeatability	0.016 deg/hr	0.007 deg/hr
Random Drift (1 σ)	0.024 deg/hr	<0.01 deg/hr
g Sensitive Drift	0.2 deg/hr/g	0.05 deg/hr/g
g Sensitive Drift Repeatability	0.016 deg/hr/g	0.007 deg/hr/g
Anisoelastic Drift	None	None
Temperature Sensitivity	0.002 deg/hr/°C	<0.002 deg/hr/°C
Magnetic Sensitivity	None	None
g Limit Capability	10 g	10 g
Reaction Time	<One Minute	<One Minute
Size	3 in. dia. x 3 in. l	3 in. dia. x 3 in. l

An alternate method of measuring the g-sensitive noise has proven very informative in examining the noise characteristics. Again the gyro is positioned with the spin axis parallel to the earth rotation vector. In this test, however, the instrument case is not continuously rotated. Instead, the instrument is indexed in 45° increments through 360° about the spin axis and the amplitude and phase of the 2ν noise is measured for each position. The variations in the 2ν are proportional to the g-sensitive noise.

Analysis of the test results show that:

a) A sideband signal is generated that is proportional to g-sensitive noise but is not at the Nutatron frequency.

b) The sideband signal tracks the g-sensitive noise to within 10% to 20% and could eventually be used as a rough measure of g-sensitive noise. While it could possibly be used as a compensation signal, the direction of the development and analysis efforts is to reduce the g-sensitive noise to a level that requires no compensation.

c) The g-sensitive noise is not a simple amplitude modulation of the 2ν noise level by the pickoffs, suspension system, electronics, etc., but rather is noise generated within the rotor/bearing structure.

d) The indexing test can be run without installing the rotor in the case. Therefore, investigation of g-sensitive noise can be done with the rotor in the open to permit easy access to the bearings, etc.

2. Cross Coupling Test

The cross coupling of noise from the spin axis into the sensitive axes was measured by temporarily adding a special pickoff to sense motions around the spin axis. By comparing the output of this pickoff to the regular pickoff, the amount of cross coupling could be measured. The test showed that much of the random noise near the Nutatron frequency appearing in the sensitive axis was cross coupled from the spin axis. It was also determined from the test that the g-sensitive noise originates directly in the sensitive axes.

3. Effect of Bearing Misalignment

Analysis of the effects of bearing misalignment showed that this could be a major source of g-sensitive noise. To confirm this, a rotor was disassembled and the bearings were realigned to improve their parallelism. Testing of the g-sensitive noise before and after reassembly showed a significant improvement in performance (factor of three). Further improvement could not be obtained on this rotor due to limitations on the parallelism achievable. As a result, the bearing mounting provisions on all subsequent rotors will be modified.

4. Randomness Investigation

Close investigation of the characteristics of the randomness of the Nutatron output revealed a low frequency periodicity. The frequency of this signal varies greatly from rotor to rotor. The source of this signal is the beating of the ball complement frequencies of the two spin bearings. The more closely matched the bearings are, the lower the beat frequency. Eventually bearings dissimilar enough to give a high frequency beat will be used so this signal can be filtered.

5. Temperature Test

(C) The internal temperature of the gyro was varied by 20°C and the various drift parameters were measured. The results showed a drift coefficient of 0.002°/hr/°C for all drift parameters. It was also shown that the bearing alignment affects the temperature coefficient of g-sensitive drift. It is anticipated that improved alignment will reduce this temperature coefficient to less than 0.001°/hr/°C.

6. Independence from Operating Parameters

(U) A series of tests were run to determine the dependence of the performance parameters on various operating conditions such as electronic loop gains, etc. The tests showed that the same performance is obtained independent of:

a) Pickoff excitation voltage
b) Pickoff gaps
c) Constrainment loop response
d) Position of the rotor in the case
e) Level of mass unbalance
f) Dynamic unbalance of the rotor
g) Housing rotation rate
h) Resonance conditions
i) Axis alignment loop response

C. Analysis of Ball Bearing Noise

(U) The analysis of ball bearing noise at twice the rotor frequency was focused on two types of geometric errors:

1. An elliptical runout of the outer (spinning) bearing race,

2. A tilt of the outer race due to mounting imperfections. The analysis showed that both of these errors produce g-sensitive noise at twice the rotor frequency. The noise arising from a mounting tilt, however, was shown to be much higher than the noise due to race imperfections. The symbols used in the analyses are listed following the Table of Contents. The details of the analysis follow.

1. Effect of Elliptical Races

(U) This analysis is simplified by the assumption that all balls remain in a state of compression for all possible conditions of loading. This requirement is satisfied in the instrument by setting an initial bearing preload of approximately 3 pounds. Intuitively, if one or more balls become unloaded during a revolution of the rotor, additional undesirable noise can be expected to appear.

(U) For calculation of displacements, the mathematical approach used was to assume a displacement, calculate the individual ball loads and sum these up to obtain the resultant loads. A digital computer was used to perform the iterative calculations.

a) Derivation of Equations

Starting with the equations for the sum of radial and axial loads (Reference 1):

$$F_r = \sum_{\psi=-\pi}^{\psi=+\pi} Q_\psi \cos\alpha \cos\psi \tag{4}$$

$$F_a = \sum_{\psi=-\pi}^{\psi=+\pi} Q_\psi \sin\alpha \tag{5}$$

The individual ball loads are found in terms of the heaviest loaded ball.

$$Q_\psi = Q_{max} \left[1 + \frac{1}{2\epsilon} \left(1 - \cos\psi \right) \right]^{3/2} \tag{6}$$

$$\epsilon = \frac{1}{2} \left(1 + \frac{\delta_a \tan\alpha}{\delta_r} \right) \tag{7}$$

In order to evaluate Q_{max}, the normal ball-race deformation, δ_{max}, is required.

$$\delta_{max} = \delta_a \sin\alpha + \delta_r \cos\alpha \tag{8}$$

$$Q_{max} = K_n \, \delta_{max}^{3/2} \tag{9}$$

K_n may be found using equations contained in Reference 1 or in Reference 2. Typically for bearings of the size used in the Nutatron, K_n varies from 0.3×10^7 to 0.5×10^7 lb/in.$^{3/2}$.

b. Calculation of Displacements

Using the foregoing equations, a computer program was written to calculate the radial motion of the bearing races relative to each other for constant radial load. The motions were calculated for a 1g radial load and for zero radial load. The difference between these yields the "g" sensitive noise attributable to race ellipticity.

Figure 3 is a flow chart illustrating the computer solution for the noise.

c. Discussion of Results

Results of the computer analysis for four types of bearings are tabulated in Table II. An elliptical error in the bearing race produces a small g-sensitive 2ν motion. The 2ν motion results

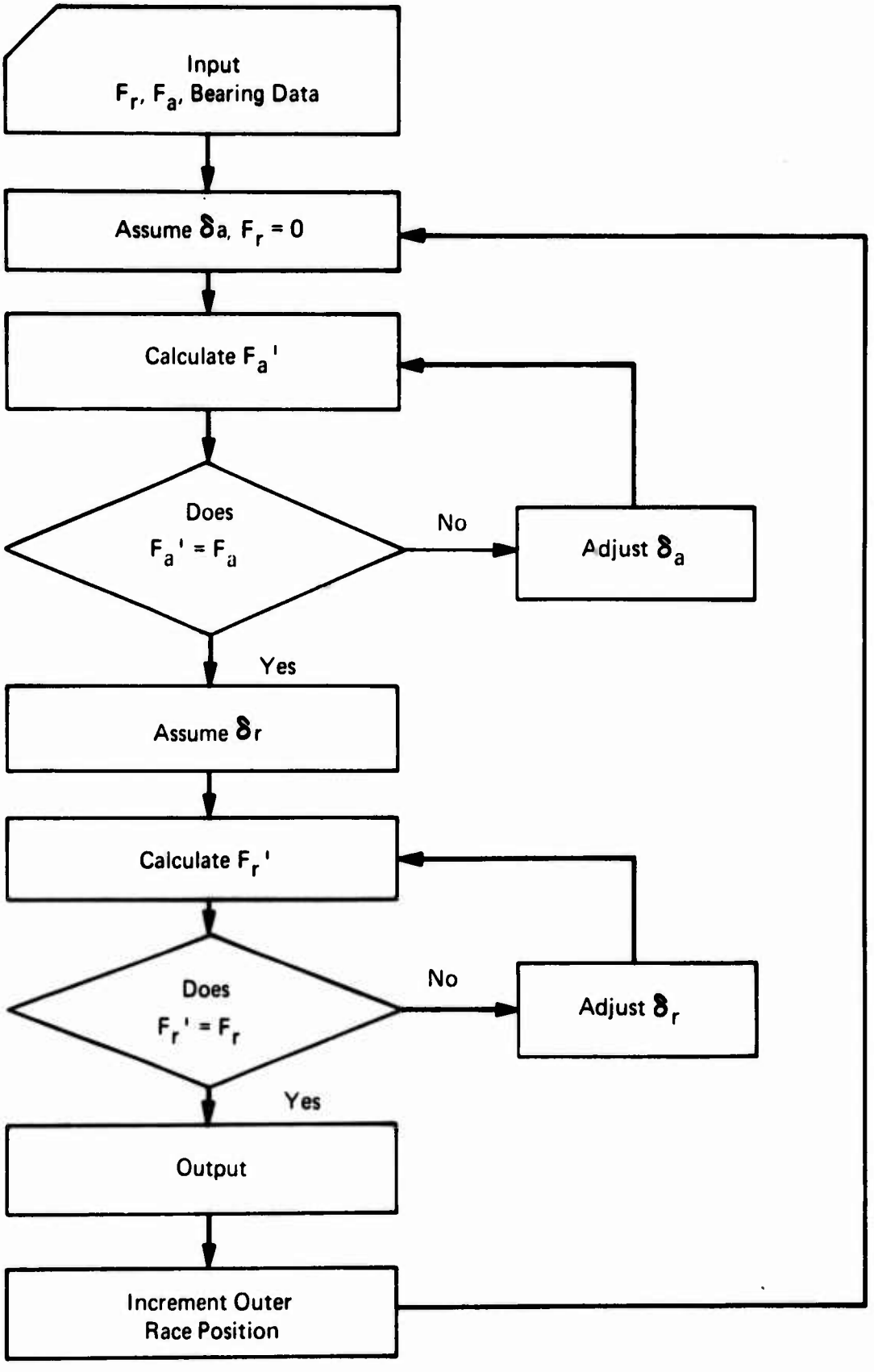

Figure 3. Flow Chart for Elliptical Race Solution

TABLE II
EFFECT OF ELLIPTICAL GEOMETRY ERRORS ON RADIAL DISPLACEMENT

Item	New Hampshire Standard	Miniature Precision Bearing Standard	New Hampshire Modified	Miniature Precision Bearing Modified
No. of Balls	8	10	11	13
Ball Size	0.0781 in.	0.0625 in.	0.0781 in.	0.0625 in.
Free Contact Angle	15.0°	15.0°	12.5°	12.5°
Typical 2 ν Noise (ν sec)	705	560	500	460

because the elliptical error produces a modulation of the spring rate at twice per revolution due to nonlinearity of the ball versus race deformation equation. However, because the bearing is preloaded, the percent modulation of the ball load is relativ ly low and the amplitude of the g-sensitive motion is small compared to the elliptical race error.

The expected geometry error to be encountered in actual bearings is difficult to predict. Usually the "out-of-round" errors are specified and measured as total errors without regard to the number of cycles around the circumference. This makes it difficult to separate the elliptical error from the other geometrical errors. Typically, an ABEC 7 bearing will be specified as being 100 microinches out of round on the inner race and 200 microinches out of round on the outer race. The bearing manufacturers contracted (New Hampshire Bearings and Miniature Precision Bearings Inc.) believe that the out-of-round errors are less than 30 microinches consisting largely of third and fifth harmonics. They declined to comment on probable amount of second harmonic as it is concealed by the odd harmonics.

2. Effect of Tilted Races

As was assumed in the analysis above, all balls remain in a state of compressive loading. The following analysis is based upon the same conditions as for the elliptical race errors so that direct comparison can be made.

a. Derivation of Equations

For calculation of the effect of a tilted race, it is necessary to use an analysis which takes into account a moment loading in addition to the axial and radial loads. The basic equations are derived in Reference 1.

The normal approach of the races, δ_n, is modified in this analysis to include a tilted outer race and angles of tilt not in the plane of the radial load. Reference 1 gives the following equation for the inner race tilted in the plane of the radial load:

$$\delta_n = A \left\{ \left[\left(\sin\alpha^\circ + \bar{\delta}_a + R_i \bar{\theta} \cos\psi \right)^2 + \left(\cos\alpha^\circ + \bar{\delta}_r \cos\psi \right)^2 \right]^{1/2} - 1 \right\} \qquad (10)$$

For a tilted outer race, R_o is substituted for R_i everywhere it appears. (R_o and R_i are the locus of centers of curvature of the bearing races.) If the outer race is tilted in a plane other than the plane of the radial displacement, the equation is modified by introducing a phase angle in the $\theta \cos\psi$ term. The normal approach equations are summarized for the various options:

Inner Race Tilted:

In Plane of Radial Load:

$$\delta_n = A \left\{ \left[\left(\sin\alpha^\circ + \bar{\delta}_a + R_i \bar{\theta} \cos\psi \right)^2 + \left(\cos\alpha^\circ + \bar{\delta}_r \cos\psi \right)^2 \right]^{1/2} - 1 \right\}$$

In Perpendicular Plane:

$$\delta_n = A \left\{ \left[\left(\sin\alpha^\circ + \bar{\delta}_a + R_i \bar{\theta} \sin\psi \right)^2 + \left(\cos\alpha^\circ + \bar{\delta}_r \cos\psi \right)^2 \right]^{1/2} - 1 \right\} \qquad (11)$$

Outer Race Tilted:

In Plane of Radial Load

$$\delta_n = A \left\{ [(\sin \alpha^\circ + \bar{\delta}_a + R_o \bar{\theta} \cos \psi)^2 + (\cos \alpha^\circ + \bar{\delta}_r \cos \psi)^2]^{1/2} - 1 \right\} \quad (12)$$

In Perpendicular Plane:

$$\delta_n = A \left\{ [(\sin \alpha^\circ + \bar{\delta}_a + R_o \bar{\theta} \sin \psi)^2 + (\cos \alpha^\circ + \bar{\delta}_r \cos \psi)^2]^{1/2} - 1 \right\} \quad (13)$$

The appropriate equation can be used to calculate the normal ball load.

$$Q = K_n \delta_n^{1.5}$$

The individual loaded ball contact angles may be found from:

$$\sin \alpha = \frac{\sin \alpha^\circ + \bar{\delta}_a + R_i \bar{\theta} \cos \psi}{[(\sin \alpha^\circ + \bar{\delta}_a + R_i \bar{\theta} \cos \psi)^2 + (\cos \alpha^\circ + \bar{\delta}_r \cos \psi)^2]^{1/2}} \quad (14)$$

$$\cos \alpha = \frac{\cos \alpha^\circ + \delta_r \cos \psi}{[(\sin \alpha^\circ + \bar{\delta}_a + R_i \bar{\theta} \cos \psi)^2 + (\cos \alpha^\circ + \bar{\delta}_r \cos \psi)^2]^{1/2}} \quad (15)$$

The appropriate substitutions for R_i and $\theta \cos \psi$ must be made as before.

To find the resultant radial, axial, and moment loads, the following summations must be performed.

$$F_a = \sum_{\psi = 0}^{\psi = 2\pi} Q_\psi \sin \alpha \quad (16)$$

$$F_r = \sum_{\psi = 0}^{\psi = 2\pi} Q_\psi \cos \psi \cos \alpha \quad (17)$$

$$M_1 = \tfrac{1}{2} d_m \sum_{\psi = 0}^{\psi = 2\pi} Q_\psi \cos \psi \sin \alpha \quad (18)$$

$$M_2 = \tfrac{1}{2} d_m \sum_{\psi=0}^{\psi=2\pi} Q_\psi \sin\psi \sin\alpha \qquad (19)$$

In most cases either M_1 or M_2 will be equal to zero.

b. Calculation of Displacements

The method of calculation was to find δ_a by iteration assuming a preload F_a and an angular tilt θ and setting $\delta_r = 0$. Then δ_r was found by iteration for a radial one "g" load and δ_a constant. A new F_a and the moments were then calculated. This computational technique is illustrated by the flow chart (Figure 4).

c. Discussion of Results

Examination of the results (Figures 5 and 6) shows a definite preponderance of 2ν noise when the non-g-sensitive noise is subtracted out. It is of interest to note that the non-g-sensitive noise is predominantly at the spin frequency while the g-sensitive noise is predominantly at 2ν. As the noise amplitude is proportional to the square of the angle of outer race tilt, it can be concluded that improvement of the alignment of the races relative to each other is of primary consideration.

D. Model Equation for Bearing Noise

The test program showed that essentially there are four types of bearing noise at the 2ν frequency.

1) g-insensitive coning noise at 2ν. This noise can be represented by a vector that rotates in the same direction as the rotor.
2) g-insensitive anticoning noise at 2ν. In this case, the noise vector rotates counter to the rotor.
3) g-sensitive 2ν noise that cones at the case rotation frequency Ω.
4) g-sensitive 2ν noise that anticones at the case rotation frequency.

For the purpose of investigating these noise components, a bearing race model equation was derived. This model demonstrates the types of errors in the bearing that are required to produce the various types of noise mentioned above. This analysis also verified to a large extent the conclusions drawn from the other bearing analyses, viz. that bearing mounting imperfections have a greater impact on Nutatron performance than geometric errors within the bearing.

The model used considers the bearing races to be distorted on their radii, and a general Fourier series representation is assumed. The spring constant between races is assumed nonlinear. The three dominant bearing race errors are shown to be:

1) An elliptical outer race distortion coupled with a first harmonic inner race distortion.
2) An elliptical outer race distortion coupled with a third harmonic inner race distortion.
3) An elliptical outer race distortion coupled with a g-sensitive displacement of outer rotor with respect to inner rotor.

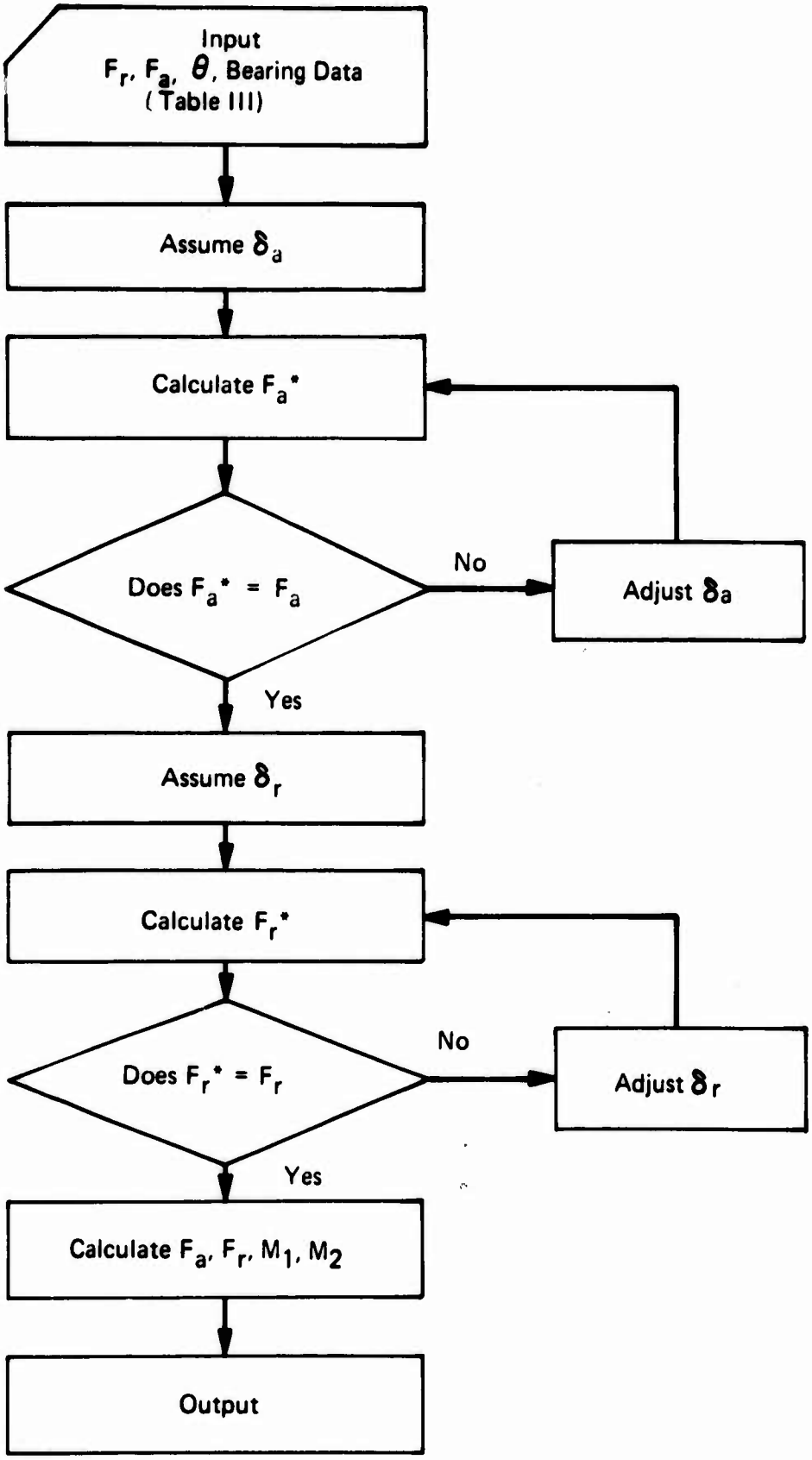

Figure 4. Flow Chart for Tilted Race Solution

TABLE III
PARAMETERS USED IN THE ANALYSIS

Bearing Data:

Mean Diameter = D_m = 0.375 in.
Ball Diameter = D = 0.0781 in.
No. of Balls = Z = 8
Free Contact Angle = α° = 15.5°
Race Curvature Ratio = f_o = f_i = 0.555
Ball/Race Spring Rate Coefficient = K_m = 0.304×10^7 lb/in.$^{3/2}$

Loads:

Preload (Axial) = F_a = 3 lb
Radial Load at 1 g = 0.165 lb
Angular Tilts = 0.0001 to 0.0005 radian

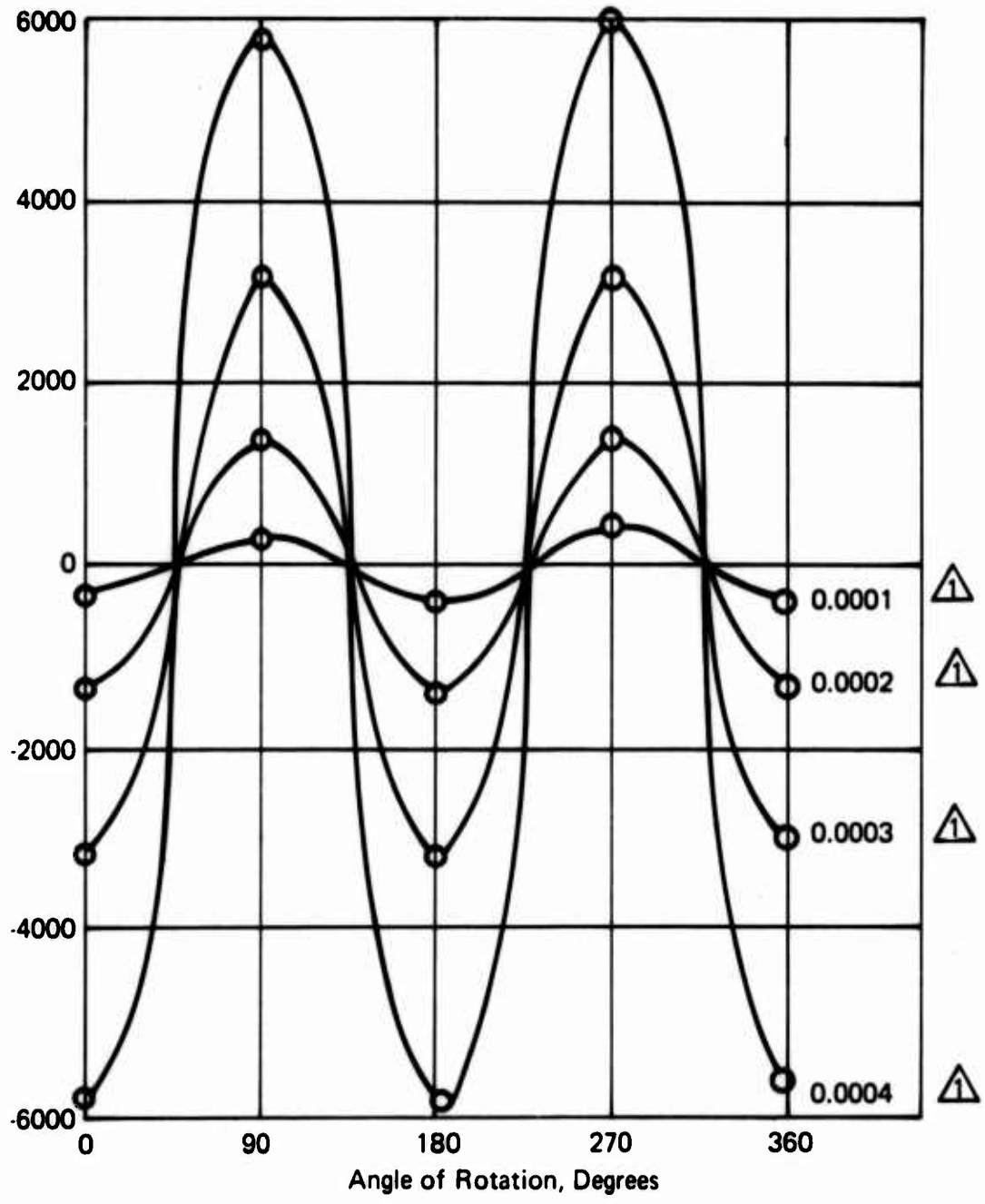

Figure 5. g - Sensitive 2ν Motions versus Angle of Rotation

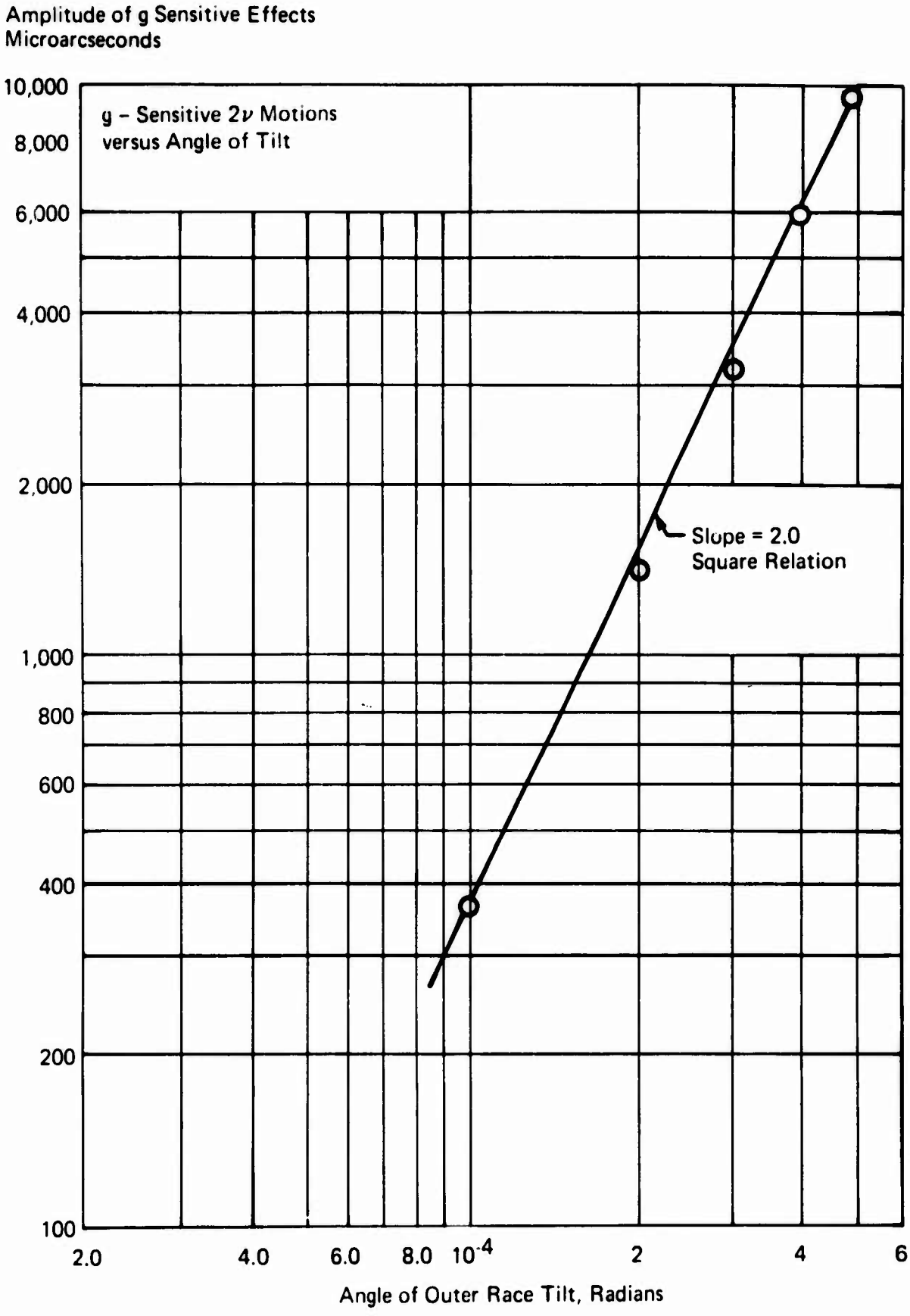

Figure 6. g - Sensitive Motions versus Angle of Tilt

The same race geometry errors give rise to both straight 2ν noise and g-modulated 2ν noise.

Only one bearing race geometry is considered; the other spin bearing is assumed ideal. The bearing outer race translational motions give rise to angular motions and the total angular motions are a superposition of the motions of both bearing outer races assuming the opposing bearing in each case to be ideal.

1. Discussion of the Results of the Analysis (Appendix A).

The bearing induced angular 2ν noise (from one bearing) can be expressed as:

$$\theta_{nx} = \frac{\pi k_2 r_{O_2}}{R K_1} \left[r_{i_3} \sin(2\nu t + \varphi_2) + \delta \sin\left(2\nu t + \Omega t + \frac{\pi}{2} - 2\beta_2\right) - r_{i_1} \sin(2\nu t + \varphi_1) \right] \left[1 + \frac{2WK_2}{K_1^2} \cos \Omega t \right] \tag{20}$$

$$\theta_{ny} = \frac{\pi k_2 r_{O_2}}{R K_1} \left[r_{i_3} \cos(2\nu t + \varphi_2) - \delta \cos\left(2\nu t + \Omega t + \frac{\pi}{2} - 2\beta_2\right) + r_{i_1} \cos(2\nu t + \varphi_1) \right] \left[1 + \frac{2WK_2}{K_1^2} \sin \Omega t \right] \tag{21}$$

where:

θ_{nx}, θ_{ny}	=	angular motions between races in the x and y axes, respectively.
R	=	distance between bearings (cm)
K_1	=	linear translation spring constant of bearing (dyne/cm)
K_2	=	Second order translational spring constant of bearing (dyne/cm^2)
k_2	=	Second order radial pressure constant of bearing (dyne/cm^2)
W	=	Rotor weight (dyne)
r_{i_1}, r_{i_3}	=	First and third harmonic distortion of inner race (cm)
r_{O_2}	=	Second harmonic distortion of outer race (cm)
δ	=	Translational displacement of outer race due to rotor weight ($\delta = \frac{W}{K_1}$) (cm)
Ωt	=	Angle of g-vector with respect to an inner race coordinate system. (The inner race is considered stationary and the g-vector rotates opposite to direction of case rotation).
φ_1	=	$\alpha_1 - 2\beta_2$
φ_2	=	$3\alpha_3 - 2\beta_2$
β_2	=	Angle of second harmonic outer race distortion
α_1	=	Angle of first harmonic inner race distortion
α_3	=	Angle of third harmonic inner race distortion

The bearing induced noise consists of a coning and an anticoning component; the terms multiplied by r_{i_1} and δ in equations (20) and (21) are coning at 2ν, whereas the terms multiplied by r_{i_3} are anticoning at 2ν.

The pickoff response to these noise inputs are:

$$\begin{bmatrix}\theta_x\\ \theta_y\end{bmatrix} = A\left\{a\, r_{i_1}\begin{bmatrix}\sin(2\nu t+\varphi_1-\eta)\\ -\cos(2\nu t+\varphi_1-\eta)\end{bmatrix} + b\, r_{i_3}\begin{bmatrix}-\sin(2\nu t+\varphi_2)\\ -\cos(2\nu t+\varphi_2)\end{bmatrix}\right\}$$

$$+\sqrt{2}\,B_2\left\{a\left(r_{i_1}\cos\phi\begin{bmatrix}\sin(2\nu t+\varphi_1-\eta)\\ -\cos(2\nu t+\varphi_1-\eta)\end{bmatrix} + r_{i_3}\sin\phi\begin{bmatrix}\sin(2\nu t+\varphi_2-\eta)\\ -\cos(2\nu t+\varphi_2-\eta)\end{bmatrix}\right.\right.$$

$$\left.-\frac{B_1}{\sqrt{2}\,B_2}\begin{bmatrix}\sin(2\nu t+\phi+\varphi_3)\\ -\cos(2\nu t+\phi+\varphi_3)\end{bmatrix}\right) \qquad (22)$$

$$\left.-b\left(r_{i_3}\cos\phi\begin{bmatrix}\sin(2\nu t+\varphi_2)\\ \cos(2\nu t+\varphi_2)\end{bmatrix} + r_{i_1}\sin\phi\begin{bmatrix}\sin(2\nu t+\varphi_1)\\ \cos(2\nu t+\varphi_1)\end{bmatrix}\right)\right\}$$

where:

$$A = \frac{2\pi k_2\, r_{O_2}}{R\,K_1}$$

$$B_1 = \frac{2\pi k_2\, W\, r_{O_3}}{R\,K_1^{\,2}}$$

$$B_2 = \frac{2\pi k_2\, W\, r_{O_2} K_2}{R\,K_1^{\,3}}$$

$$a = \frac{\nu^2\,\Delta'}{\sqrt{(K-2\nu^2\,\Delta)^2+4\nu^2\,R_d^{\,2}}}$$

$$b = \frac{\nu^2\,(2C+\Delta')(1+N)}{K-2\nu^2\,(2C+\Delta)(1+P)}$$

$$\Delta' = A+B-C$$

$$\Delta = A+B-C+2I$$

ν = operating speed

K = pivot spring constant

A,B,C = rotor inertias

I = non-rotating inertia

R_d = damping constant

$$\eta = \tan^{-1}\frac{2\nu R_d}{K-2\nu^2\Delta}$$

P, N = rotor geometry constants

$$\phi = \Omega t - \frac{\pi}{4}$$

$$\varphi_3 = \frac{3\pi}{4} - 2\beta_2$$

The terms multiplied by A are non-g-sensitive 2ν responses. The term multiplied by r_{i_1} cones at 2ν, whereas the term multiplied by r_{i_3} anticones at 2ν. The terms multiplied by $\sqrt{2}\,B_2$ are g-sensitive 2ν responses. Of these, the terms multiplied by the constant, a, cone at 2ν and the terms multiplied by b anticone at 2ν.

As the case is rotated through 360°, Ωt moves from 0 to 360° or ϕ rotates from −45° to 315°. The resultant ellipses in the x and y axes when plotted in polar coordinates either cone or anticone depending on the relative magnitudes of r_{i_1}, r_{i_3} and $B_1/\sqrt{2}\,B_2$, and on the relationship between the phase angles, φ_1, φ_2, φ_3 and η. For example, let us assume that $B_1 = 0 = b$, then the pick off responses reduce to:

$$\begin{bmatrix}\theta_x\\ \theta_y\end{bmatrix} = A\,a\,r_{i_1}\begin{bmatrix}\sin(2\nu t+\varphi_1-\eta)\\ -\cos(2\nu t+\varphi_1-\eta)\end{bmatrix} + \sqrt{2}\,B_2\,a\left\{r_{i_1}\cos\phi\begin{bmatrix}\sin(2\nu t+\varphi_1-\eta)\\ -\cos(2\nu t+\varphi_1-\eta)\end{bmatrix} + r_{i_3}\sin\phi\begin{bmatrix}\sin(2\nu t+\varphi_2-\eta)\\ -\cos(2\nu t+\varphi_2-\eta)\end{bmatrix}\right\} \tag{23}$$

The first term is a resonant non-g-sensitive 2ν noise. The second term represents a resonant coning or anticoning ellipse when these responses are demodulated at 2ν. If φ_1 and φ_2 are in the same half plane ($< 90°$ apart), the resultant ellipse cones with respect to the case angle, $\Omega t = \phi + \pi/4$. Conversely, if φ_1 and φ_2 are in opposite half planes ($> 90°$ apart) the resultant ellipse anticones. If $r_{i_1} = r_{i_3}$ and $\varphi_1 = \varphi_2$, the result is a coning circle, and if $\varphi_1 = \varphi_2 + \pi$, the result is an anticoning circle.

In the above example we have assumed that the term multiplied by B_1 is negligible. This term is a direct g-sensitive noise which cones both at 2ν and Ω. The ratio $B_1/\sqrt{2}\,B_2 = K_1/\sqrt{2}\,K_2 = r_o$ has the dimensions of length. When this term is included with the other terms multiplied by the resonant factor, a, it is difficult to predict the necessary relative magntiudes of r_{i_1}, r_{i_3} and r_o, and the relative phase angles φ_1, φ_2 and φ_3 for coning or anticoning at Ω.

The terms multiplied by b are nonresonant, anticoning (at 2ν) responses. For the non-g-sensitive part of the response (terms multiplied by A in Equation (22)), the part of the response multiplied by b gives non-g-sensitive vectors (after demodulation at 2ν) which are not at right angles in the x and y axes. The tangent of the angle between these vectors can be expressed as:

$$\tan(\theta_y - \theta_x) = \frac{A_1^2 - A_2^2}{2A_1A_2\sin(\varphi_2 - \varphi_1 + \eta)} \tag{24}$$

where

θ_x, θ_y	=	polar angles of x and y axis vectors
A_1	=	$A\, r_{i_1}\, a$
A_2	=	$A\, r_{i_3}\, b$

$\theta_y - \theta_x = 90°$ only if either $A_2 = 0$ or $\varphi_1 = \varphi_2 + \eta$. If $A_2 \neq 0$, there exists an anticoning component at 2ν. In this model, the anticoning component is proportional to r_{i_3} and is not resonance amplified, whereas, the coning component is proportional to r_{i_1} and is resonance amplified. The non perpendicularity of the two non-g-sensitive noise vectors depends on the relation between A_1 and A_2 or in part on the relation between the nonresonant response gain, b and the resonant gain, a.

The inner race distortions can possibly be caused by a bump or a series of bumps. Assume the inner race distortion is caused by one bump which can be represented by the peak of a sine wave as illustrated in Figure 7. If the circle is opened as shown in Figure 8, a Fourier series can be written for the harmonic content of the bump:

$$r = \frac{A}{\pi\left(1-\cos\frac{\phi}{2}\right)}\left[\left(\sin\frac{\phi}{2}-\frac{\phi}{2}\cos\frac{\phi}{2}\right)+\left(\frac{\phi}{2}-\sin\frac{\phi}{2}\cos\frac{\phi}{2}\right)\cos\theta\right.$$

$$\left.+\ldots+\left(\frac{\sin(n+1)\frac{\phi}{2}}{n+1}+\frac{\sin(n-1)\frac{\phi}{2}}{n-1}-2\sin\frac{n\phi}{2}\cos\frac{n\phi}{2}\right)\cos n\theta+\ldots\right] \qquad (25)$$

where

ϕ	=	segment angle of bump
A	=	height of bump
θ	=	angle of fundamental wave period

We are interested in the amplitudes of the fundamental and third harmonic of the fundamental.

1st: $$\frac{\phi}{2}-\sin\frac{\phi}{2}\cos\frac{\phi}{2}\;\frac{A}{\pi\left(1-\cos\frac{\phi}{2}\right)}$$

3rd: $$\left(\frac{\sin 2\phi}{4}+\frac{\sin\phi}{2}-\frac{2\sin\frac{3\phi}{2}\cos\frac{\phi}{2}}{3}\right)\frac{A}{\pi\cos\frac{\phi}{2}}$$

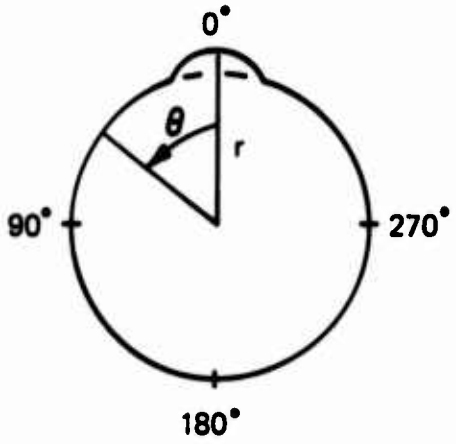

Figure 7. Bump on Inner Race

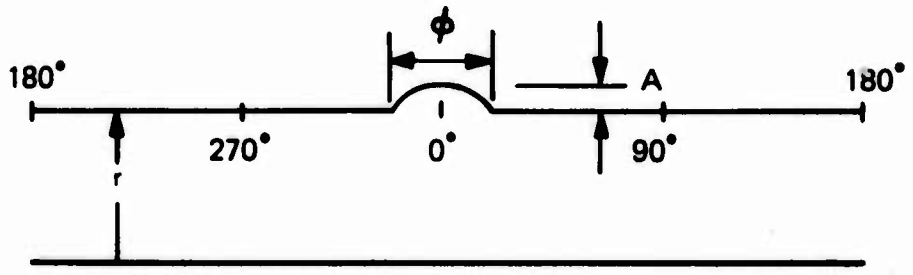

Figure 8. Circle with Bump Opened Up

Assume ϕ to be small enough such that $\cos\phi = 1 - \frac{\phi^2}{2}$ and $\sin\phi = \phi - \frac{\phi^3}{6}$, then the Fourier amplitudes are:

$$\text{1st:} \quad \left[\frac{\phi}{2} - \left(\frac{\phi}{2} - \frac{\phi^3}{48}\right)\left(1 - \frac{\phi^2}{8}\right)\right] \frac{A}{\pi\frac{\phi^2}{8}} \cong \frac{\phi^3 A\, 8}{12\pi\phi^2} = \frac{2}{3}\frac{A\phi}{\pi}$$

$$\text{3rd:} \quad \frac{2\phi - \frac{8\phi^3}{6}}{4} + \frac{\phi - \phi^3}{\frac{6}{2}} - \frac{2}{3}\left(\frac{3\phi}{2} - \frac{27}{48}\phi^3\right)\left(1 - \frac{\phi^2}{8}\right) \frac{A}{\frac{\pi\phi^2}{8}} \cong \frac{\phi^3 A\, 8}{12\pi\phi^2} = \frac{2}{3}\frac{A\phi}{\pi}$$

for small θ, the fundamental and third harmonic Fourier amplitudes are equal and in phase.

In a practical bearing, one would not expect a single bump on the inner race but a continuous distortion around the perimeter of the race. Based on the analysis of the single bump, however, one would expect the amplitudes of the fundamental and third harmonic distortion to be within the same order of magnitude.

The validity of this analysis depends on the following bearing errors:

(1) fundamental geometry errors on inner race (bump)
(2) third harmonic geometry errors on inner race
(3) second harmonic geometry errors of outer race
(4) g-sensitive relative translation of races
(5) a second-order bearing translational spring constant.

There is no question concerning the existence of the first four. From theoretical bearing studies, there is a question regarding the existence of a second-order bearing translational spring constant of the order necessary to give the 2ν noise levels observed during the test program. The second order spring constant necessary to produce performance errors of the magnitude of those observed in test is 100 times what is felt to be a reasonable value. Therefore, it can be concluded that the noise due to geometric errors in the bearing races is at least one order of magnitude, and very nearly two orders, below the present performance level. Furthermore, the use of special made ultrahigh precision bearings is unnecessary because the precision of conventional instrument bearings is sufficient for a high performance Nutatron.

E. Gas Bearing Study

The long life and low random noise level inherent in a gas lubricated bearing made the application of a gas bearing to the Nutatron look attractive. For this reason, the initial work statement for this contract included the design, fabrication and test of a low speed hydrodynamic gas bearing for the Nutatron rotor. Due to a change in the funding status of the contract, only the preliminary design effort was completed.

1. Methods of Analysis

The original method of analysis of the gas bearings was adapted from the thrust bearing analysis contained ... References 3 and 4. Later developments in the field of gas bearings permitted

(U)the use of the design charts contained in Reference 5. As can be seen from Table IV.5, the simplified approach is adequate for most practical design calculations.

(U) A disadvantage of the design charts is that the geometries are optimized for maximum stiffness and for isoelastic rotor support. This limits their use for optimizing 2ν noise levels at the expense of isoelasticity.

2. Gas Bearing Design

(U) The preferred configuration for a gas lubricated spin bearing is a co-apex opposed conical configuration. This configuration provides a design in which the air gap is insensitive to temperature differences and in general minor geometrical variations will affect both radial and axial loads in the same manner. The spiral groove type of bearing was selected because the average support pressures are higher than for other types. These higher support pressures yield higher load capacities, lower noise levels and smaller radial and axial displacements.

(C) The design parameters contained in Table IV were obtained by using the following initial figures:

Ambient Pressure	1.02×10^6 dyne/cm^2
Equivalent Gap	1.27×10^{-4} cm
Outside Radius	1.22 cm
Inside Radius	0.648 cm
Gas Viscosity	1.4×10^{-4} dyne sec/cm^2
Rotor speed	105 rad/sec

These figures were based on using the largest bearing geometry that would fit in the present Nutatron housing, the minimum practical running clearance (50 μ in) and the slowest practical running speed (1000 rpm).

TABLE IV
NUTATRON GAS BEARING PARAMETERS

Parameter	Calculated BAC No. 60003-142	From MTI 68TR29
1. Spiral Groove Angle	75°	72.3°
2. Groove Depth Ratio	2.0	2.06
3. Axial Spring Constant	2.6×10^{10} dynes/cm	1.43×10^{10} dynes/cm
4. Groove Length Ratio	0.7	0.7
5. Attitude Angle	N.A.	27°
6. Anisoelastic Apex Angle	35.3°	32.5°
7. Groove Depth	2.54×10^{-4} cm	2.62×10^{-4} cm

SECTION IV

CONCLUSIONS AND RECOMMENDATIONS

The analyses and investigative tests conducted under this program have produced the following significant conclusions and recommendations:

A. Conclusions

1. Expensive special made bearings are unnecessary because noise due to imperfections in the ball bearing races is not limiting the instrument performance.

2. G-sensitive Nutatron noise results from improper bearing alignment.

3. Proper bearing alignment can be achieved without increasing the instrument complexity.

4. Cross coupling of noise from the spin axis into the input axes can be eliminated by using more compliant flex leads.

5. By using two spin bearings with different ball complement speeds, the beat frequency component of the randomness can be eliminated.

6. After modifying the engineering model as indicated above, it will be ready for test at Holloman AFB (or any other suitable facility).

7. A low speed gas bearing is feasible.

8. A thorough noise study is necessary before a gas bearing is incorporated.

B. Recommendations

1. Modify the Nutatron rotor structure to insure proper bearing alignment.

2. Incorporate flex leads that are very compliant.

3. Use spin bearings with slightly different contact angles to eliminate beat frequency problem.

4. Evaluate the modified engineering model Nutatron at an independent test facility such as Holloman AFB.

5. Incorporation of a low speed gas bearing should be postponed pending further investigation.

APPENDIX A

Analysis of a Bearing Model Equation

Referring to Figure 9, let the inner race be stationary with an x-y coordinate system tied to it. The outer race rotates CCW at ν and let the g-vector rotate clockwise at Ω. (Corresponds to a CCW case rotation.)

$$\text{Let } r_i = r_{i_0} + r_{i_1} \cos(\theta + \alpha_1) + r_{i_2} \cos 2(\theta + \alpha_2) + r_{i_3} \cos 3(\theta + \alpha_3) + \ldots$$

$$r_O = r_{i_0} + d + r_{O_1} \cos(\theta_O + \beta_1) + r_{O_2} \cos 2(\theta_O + \beta_2) + r_{O_3} \cos 3(\theta_O + \beta_3) + \ldots$$

$$+ \delta \cos(\theta - \psi)$$

where

r_{i_0}	=	nominal inner race radius
d	=	ball diameter
r_{ij}	=	j^{th} harmonic distortion of inner race radius
r_{oj}	=	j^{th} harmonic distortion of outer race radius
αj	=	j^{th} distortion phase angle of inner race
βj	=	j^{th} distortion phase angle of outer race
δ	=	outer rotor displacement from rotor weight
W	=	rotor weight
ψ	=	angle of g-vector
θ	=	angle variable in stationary coordinates
ν	=	angular velocity of outer race
Ω	=	angular velocity of g-vector

The outer race is moving CCW, then the instantaneous gap between races as a function of θ is

$$\Delta r = r_O - r_i \text{ and } \theta_O = \theta - \nu t$$

Assume a linear continuous pressure distribution radially outward on the outer race according to the equation:

$$p_r = p_0 + p_1 (r_i - r_O + d) + p_2 (r_i - r_O + d)^2 + p_3 (r_i - r_O + d)^3 + \ldots \quad (26)$$

Then the incremental radial outward force is:

$$df_r = p_r r_{oo} d\theta$$

where

r_{oo}	=	$r_{io} + d$ is the nominal outer race radius
p_O	=	radial preload pressure
p_j	=	j^{th} order of radial pressure
Let k_j	=	$r_{oo} p_j$ be the j^{th} order of radial spring constant.

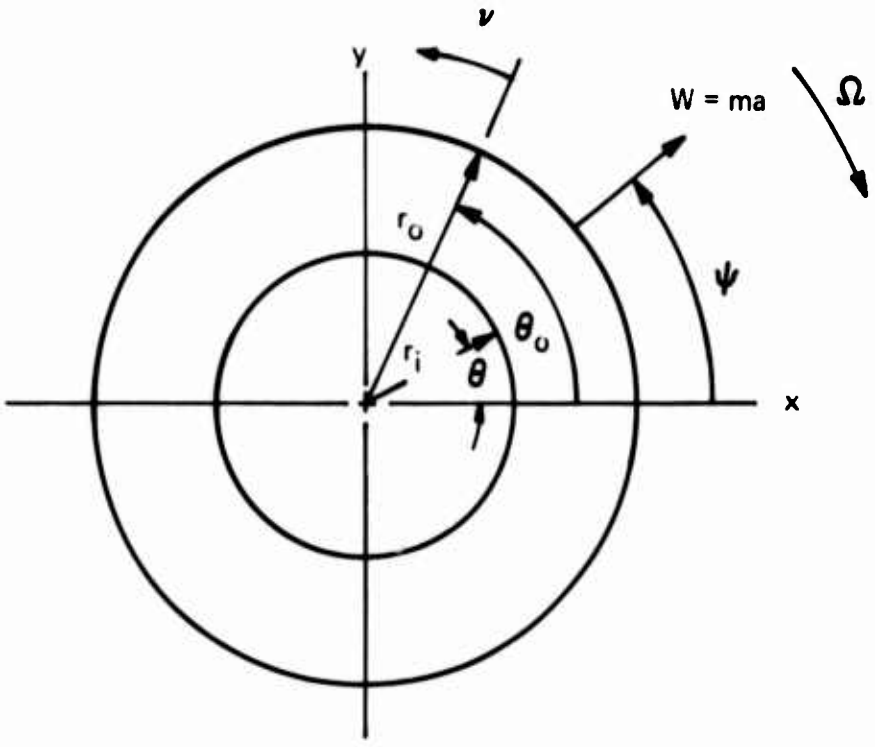

Figure 9. Sketch of Geometry of Inner and Outer Bearing Race

Then expanding

$$
\begin{aligned}
df_r = \{ & k_0 + k_1 [r_{i_1} \cos(\theta + \alpha_1) - r_{o_1} \cos(\theta + \beta_1 - \nu t) \\
& + r_{i_2} \cos 2(\theta + \alpha_2) - r_{o_2} \cos 2(\theta + \beta_2 - \nu t) \\
& + r_{i_3} \cos 3(\theta + \alpha_3) - r_{o_3} \cos 3(\theta + \beta_3 - \nu t) + \ldots \\
& + \delta \cos(\theta - \psi)] \\
& + k_2 [r_{i_1} \cos(\theta + \alpha_1) - r_{o_1} \cos(\theta + \beta_1 - \nu t) \\
& + r_{i_2} \cos 2(\theta + \alpha_2) - r_{o_2} \cos 2(\theta + \beta_2 - \nu t) \\
& + r_{i_3} \cos 3(\theta + \alpha_3) - r_{o_3} \cos 3(\theta + \beta_3 - \nu t) + \ldots \\
& + \delta \cos(\theta - \psi)]^2 \\
& + k_3 [\ldots]^3 + \ldots \} d\theta
\end{aligned}
\tag{27}
$$

We are interested only in force terms which give rise to translational motions of the outer race with respect to the inner. The net forces along the x and y axes are found by intergrating on θ from 0 to 2π as follows:

$$
\begin{aligned}
f_x &= \int_0^{2\pi} \frac{df_r}{d\theta} \cos\theta \, d\theta + W \cos\psi \\
f_y &= \int_0^{2\pi} \frac{df_r}{d\theta} \sin\theta \, d\theta + W \sin\psi
\end{aligned}
\tag{28}
$$

where

ψ = $-(\Omega t + \pi/2)$*
f_x = x-axis force
f_y = y-axis force

Since $df_r/d\theta$ is multiplied by either $\cos\theta$ or $\sin\theta$ in equation (28), the integrals are non-zero only when the terms in $df_r/d\theta$ are also multiplied by either $\cos\theta$ or $\sin\theta$. Further, only terms containing $2\nu t$ are to be considered. The first few of the terms meeting these requirements are:

$$
\begin{aligned}
\frac{df_r'}{d\theta} = \{ & -2 k_2 [r_{i_1} \cos(\theta + \alpha_1) r_{o_2} \cos 2(\theta + \beta_2 - \nu t) \\
& + r_{i_3} \cos 3(\theta + \alpha_2) r_{o_2} \cos 2(\theta + \beta_2 - \nu t) \\
& - \delta \cos(\theta + \Omega t + \tfrac{\pi}{2}) r_{o_2} \cos 2(\theta + \beta_2 - \nu t)] \\
& + 3 k_3 [r_{i_1} \cos(\theta + \alpha_1) r_{o_1}^2 \cos^2(\theta + \beta_1 - \nu t) \\
& + r_{i_3} \cos 3(\theta + \alpha_3) r_{o_1}^2 \cos^2(\theta + \beta_1 - \nu t) \\
& + \delta \cos(\theta - \psi) r_{o_1}^2 \cos^2(\theta + \beta_1 - \nu t)] \}
\end{aligned}
\tag{29}
$$

*At t = 0, the g-vector is assumed downward. The g-vector rotates clockwise.

If the geometry radius errors are assumed small, only the terms multiplied by k_2 need be considered. Expanding these and ignoring terms involving 3θ we have

$$\begin{aligned}
\frac{df_r'''}{d\theta} &= -k_2 [r_{i_1} r_{o_2} \cos(\theta + 2\beta_2 - \alpha_1 - 2\nu t) \\
&\quad + r_{i_3} r_{o_2} \cos(\theta + 3\alpha_3 - 2\beta_2 + 2\nu t) \\
&\quad - \delta r_{o_2} \cos(\theta + 2\beta_2 - \Omega t - \tfrac{\pi}{2} - 2\nu t)] \\
&= -k_2 \Big\{ [r_{i_1} r_{o_2} \cos(2\nu t + \varphi_1) + r_{i_3} r_{o_2} \cos(2\nu t + \varphi_2) \\
&\quad - \delta r_{o_2} \cos(2\nu t + \Omega t + \tfrac{\pi}{2} - 2\beta_2)] \cos\theta \\
&\quad + [r_{i_1} r_{o_2} \sin(2\nu t + \varphi_1) - r_{i_3} r_{o_2} \sin(2\nu t + \varphi_2) \\
&\quad - \delta r_{o_2} \sin(2\nu t + \Omega t + \tfrac{\pi}{2} - 2\beta_2)] \sin\theta \Big\}
\end{aligned} \tag{30}$$

where

$$\varphi_1 = \alpha_1 - 2\beta_2$$
$$\varphi_2 = 3\alpha_3 - 2\beta_2$$

since

$$\int_0^{2\pi} \cos^2\theta \, d\theta = \int_0^{2\pi} \sin^2\theta \, d\theta = \pi$$

and $$\int_0^{2\pi} \cos\theta \sin\theta \, d\theta = 0$$

$$\begin{aligned}
f_x &= -\pi k_2 r_{o_2} [r_{i_1} \cos(2\nu t + \varphi_1) + r_{i_3} \cos(2\nu t + \varphi_2) \\
&\quad - \delta \cos(2\nu t + \Omega t - 2\beta_2)] + W \cos(\Omega t + \tfrac{\pi}{2})
\end{aligned} \tag{31}$$

$$\begin{aligned}
f_y &= -\pi k_2 r_{o_2} [r_{i_1} \sin(2\nu t + \varphi_1) - r_{i_3} \sin(2\nu t + \varphi_2) \\
&\quad - \delta \sin(2\nu t + \Omega t - 2\beta_2)] - W \sin(\Omega t + \tfrac{\pi}{2})
\end{aligned}$$

The outer race motions caused by the forces in equation (31) are determined by the effective spring constant of the bearing. (Inertial and damping forces are considered negligible compared to the spring forces.) Assume the motion of the outer race to be defined by the equations

$$\begin{aligned}
f_x &= K_1 \delta_x + K_2 \delta_x^2 + \ldots \\
f_y &= K_1 \delta_y + K_2 \delta_y^2 + \ldots
\end{aligned} \tag{32}$$

If higher order than the 2nd are neglected, we can solve equation (32) for δ_x and δ_y.

$$\delta_x = -\frac{K_1}{2K_2} + \frac{K_1}{2K_2}\sqrt{1 + 4\frac{K_2 f_x}{K_1^2}} \approx \frac{f_x}{K_1} - \frac{f_x^2 K_2}{K_1^3} \tag{33}$$

$$\delta_y \approx \frac{f_y}{K_1} - \frac{f_y^2 K_2}{K_1^3}$$

The first terms on the right hand side of equation (33) give rise to non-g-sensitive 2ν motions and the 2nd terms give rise to g-sensitive 2ν motions by virtue of the cross product terms (W-terms) when f_x and f_y are squared. Including only the dominant terms at 2ν and 2ν modulated at Ω we have

$$\delta_x = \frac{-\pi k_2 r_{o_2}}{K_1}\left[r_{i_1}\cos(2\nu t + \varphi_1) + r_{i_3}\cos(2\nu t + \varphi_2) - \delta\cos\left(2\nu t + \Omega t + \frac{\pi}{2} - 2\beta_2\right)\right]\left(1 + \frac{2WK_2}{K_1^2}\sin\Omega t\right)$$

$$\delta_y = \frac{-\pi k_2 r_{o_2}}{K_1}\left[r_{i_1}\sin(2\nu t + \varphi_1) - r_{i_3}\sin(2\nu t + \varphi_2) - \delta\sin\left(2\nu t + \Omega t + \frac{\pi}{2} - 2\beta_2\right)\right]\left(1 + \frac{2WK_2}{K_1^2}\cos\Omega t\right) \tag{34}$$

The relationships between angular motions and the linear motions are

$$\theta_{nx} = \frac{\delta_y}{R}$$

$$\theta_{ny} = -\frac{\delta_x}{R} \tag{35}$$

where R = radius arm to opposing bearing. The bearing noise angles are

$$\theta_{nx} = \frac{\pi k_2 r_{o_2}}{R K_1}\left[r_{i_3}\sin(2\nu t+\varphi_2) - r_{i_1}\sin(2\nu t+\varphi_1) + \delta\sin\left(2\nu t+\Omega t+\frac{\pi}{2}-2\beta_2\right)\right]\left(1+\frac{2WK_2}{K_1^2}\cos\Omega t\right) \tag{36a}$$

$$\theta_{ny} = \frac{\pi k_2 r_{o_2}}{R K_1}\left[r_{i_3}\cos(2\nu t+\varphi_2) + r_{i_1}\cos(2\nu t+\varphi_1) - \delta\cos\left(2\nu t+\Omega t+\frac{\pi}{2}-2\beta_2\right)\right]\left(1+\frac{2WK_2}{K_1^2}\sin\Omega t\right) \tag{36b}$$

These are equations (1) and (2) in Section II.

The pickoff responses to the inputs can be found easiest by first transforming the noise angles into rotating rotor coordinates. Considering the non-g-sensitive noise first, the bearing noise in rotating coordinates is

$$\begin{bmatrix}\theta'_{nx}\\ \theta'_{ny}\end{bmatrix}_{2\nu} = \begin{bmatrix}\cos\nu t & \sin\nu t\\ -\sin\nu t & \cos\nu t\end{bmatrix}\begin{bmatrix}\theta_{nx}\\ \theta_{ny}\end{bmatrix}_{2\nu} = \frac{A}{2}\left\{r_{i_3}\begin{bmatrix}\cos 3\nu t & \sin 3\nu t\\ -\sin 3\nu t & \cos 3\nu t\end{bmatrix}\begin{bmatrix}\cos\left(\frac{\pi}{2}-\varphi_2\right)\\ \sin\left(\frac{\pi}{2}-\varphi_2\right)\end{bmatrix} + r_{i_1}\begin{bmatrix}\cos\nu t & -\sin\nu t\\ \sin\nu t & \cos\nu t\end{bmatrix}\begin{bmatrix}\cos\left(\varphi_1+\frac{\pi}{2}\right)\\ \sin\left(\varphi_1+\frac{\pi}{2}\right)\end{bmatrix}\right\} \tag{37}$$

where $A = \dfrac{2\pi k_2 r_{o_2}}{R K_1}$

We may write the pickoff response as

$$\begin{bmatrix}\theta_x\\ \theta_y\end{bmatrix} = A\left\{a\, r_{i_1}\begin{bmatrix}\sin(2\nu t+\varphi_1-\eta)\\ -\cos(2\nu t+\varphi_2-\eta)\end{bmatrix} - b\, r_{i_3}\begin{bmatrix}\sin(2\nu t+\varphi_2)\\ \cos(2\nu t+\varphi_2)\end{bmatrix}\right\} \tag{38}$$

where

$$a = \frac{\nu^2\Delta'}{\left[(K-2\nu^2\Delta)^2+4\nu^2 R_d^2\right]^{1/2}}\text{, the resonant gain}$$

$$b = \frac{\nu^2(2C+\Delta')(1+N)}{K-2\nu^2(2C+\Delta)(1+P)}\text{, the nonresonant gain}$$

These are the non-g-sensitive parts of Equation (22) Section II.D.

Considering next the g-sensitive terms in rotating coordinates, we have

$$\begin{bmatrix}\theta'_{nx}\\ \theta'_{ny}\end{bmatrix}_{2\nu\pm\Omega} = \begin{bmatrix}\cos\nu t & \sin\nu t\\ -\sin\nu t & \cos\nu t\end{bmatrix}\begin{bmatrix}\theta_{nx}\\ \theta_{ny}\end{bmatrix}_{2\nu\pm\Omega}$$

$$= \frac{\sqrt{2}\,B_2}{2}\left\{ r_{i_3}\begin{bmatrix}\sin(3\nu t+\varphi_2)\sin\left(\Omega t+\frac{\pi}{4}\right)+\sin(\nu t+\varphi_2)\sin\left(\Omega t+\frac{3\pi}{4}\right)\\ \cos(3\nu t+\varphi_2)\sin\left(\Omega t+\frac{\pi}{4}\right)-\cos(\nu t+\varphi_2)\sin\left(\Omega t+\frac{3\pi}{4}\right)\end{bmatrix}\right.$$

$$\left. + r_{i_1}\begin{bmatrix}-\sin(3\nu t+\varphi_1)\sin\left(\Omega t+\frac{3\pi}{4}\right)-\sin(\nu t+\varphi_1)\sin\left(\Omega t+\frac{\pi}{4}\right)\\ -\cos(3\nu t+\varphi_1)\sin\left(\Omega t+\frac{3\pi}{4}\right)+\cos(\nu t+\varphi_1)\sin\left(\Omega t+\frac{\pi}{4}\right)\end{bmatrix}\right\}$$

$$+\frac{B_1}{2}\begin{bmatrix}\sin\left(\nu t+\Omega t+\frac{\pi}{2}-2\beta_2\right)\\ -\cos\left(\nu t+\Omega t+\frac{\pi}{2}-2\beta_2\right)\end{bmatrix}$$

Let $\phi = \Omega t - \frac{\pi}{4}$

Then $\sin\left(\Omega t+\frac{\pi}{4}\right) = \cos\phi\ ;\ \sin\left(\Omega t+\frac{3\pi}{4}\right) = -\sin\phi$

$$\begin{bmatrix}\theta'_{nx}\\ \theta'_{ny}\end{bmatrix} = \frac{\sqrt{2}\,B_2}{2}\left\{\begin{bmatrix}\cos 3\nu t & \sin 3\nu t\\ -\sin 3\nu t & \cos 3\nu t\end{bmatrix}\left(r_{i_3}\cos\phi\begin{bmatrix}\cos\left(\frac{\pi}{2}-\varphi_2\right)\\ \sin\left(\frac{\pi}{2}-\varphi_2\right)\end{bmatrix}\right.\right.$$

$$\left. + r_{i_1}\sin\phi\begin{bmatrix}\cos\left(\frac{\pi}{2}-\varphi_1\right)\\ \sin\left(\frac{\pi}{2}-\varphi_1\right)\end{bmatrix}\right) + \begin{bmatrix}\cos\nu t & -\sin\nu t\\ \sin\nu t & \cos\nu t\end{bmatrix}$$

$$\left.\left(r_{i_3}\sin\phi\begin{bmatrix}\cos\left(\varphi_2+\frac{\pi}{2}\right)\\ \sin\left(\varphi_2+\frac{\pi}{2}\right)\end{bmatrix} + r_{i_1}\cos\phi\begin{bmatrix}\cos\left(\varphi_1+\frac{\pi}{2}\right)\\ \sin\left(\varphi_1+\frac{\pi}{2}\right)\end{bmatrix}\right)\right\} \qquad (39)$$

$$+\frac{B_1}{2}\begin{bmatrix}\cos\nu t & -\sin\nu t\\ \sin\nu t & \cos\nu t\end{bmatrix}\begin{bmatrix}\cos\left(\phi+\frac{\pi}{4}-2\beta_2\right)\\ \sin\left(\phi+\frac{\pi}{4}-2\beta_2\right)\end{bmatrix}$$

The pickoff response is

$$\begin{bmatrix}\theta_x\\ \theta_y\end{bmatrix}_{2\nu\pm\Omega} = a\left\{\sqrt{2}\,B_2\left(r_{i_1}\cos\phi\begin{bmatrix}\sin(2\nu t+\varphi_1-\eta)\\ -\cos(2\nu t+\varphi_1-\eta)\end{bmatrix}\right.\right. \tag{40}$$

$$\left.\left. + r_{i_3}\sin\phi\begin{bmatrix}\sin(2\nu t+\varphi_2-\eta)\\ -\cos(2\nu t+\varphi_2-\eta)\end{bmatrix}\right) - B_1\begin{bmatrix}\sin(2\nu t+\phi+\varphi_3)\\ -\cos(2\nu t+\phi+\varphi_3)\end{bmatrix}\right\}$$

$$-b\sqrt{2}\,B_2\left\{r_{i_3}\cos\phi\begin{bmatrix}\sin(2\nu t+\varphi_2)\\ \cos(2\nu t+\varphi_2)\end{bmatrix} + r_{i_1}\sin\phi\begin{bmatrix}\sin(2\nu t+\varphi_1)\\ \cos(2\nu t+\varphi_1)\end{bmatrix}\right\}$$

where $B_1 = \dfrac{2\pi k_2 W r_{O_2}}{R K_1^2}$ $\qquad \varphi_1 = \alpha_1 - 2\beta_2$

$\varphi_2 = 3\alpha_3 - 2\beta_2$

$B_2 = \dfrac{2\pi k_2 K_2 W r_{O_2}}{R K_1^3}$ $\qquad \varphi_3 = \dfrac{3\pi}{4} - 2\beta_2$

$\phi = \Omega t - \dfrac{\pi}{4}$

These are the g-sensitive portions of Equation (22) Section II.D.

The angle η is included in the trigonometric terms which are multiplied by the constant, a. This constant resonates depending on the spring compensation. If the system were undamped, a would assume a positive or negative value depending on the magnitude of $2\nu^2\Delta$ relative to K. Near resonance, a approaches $-90°$ in phase. To account for the phase shift in a, we can use the results of a previous analysis on Nutatron damping. These results show that a can be considered a positive constant plus a lagging phase angle included in all associated trigonometric terms. For small pivot spring constants, the phase of a approaches $-180°$; therefore, $\eta \to 180°$. At resonance, $\eta = 90°$, and for large K, $\eta \to 0°$. The constant, b, is also modified somewhat by the damping constant, R, but this term is far from any resonance; hence $b < 0$ can be calculated with sufficient accuracy independent of R.

In practice, the pickoff signals are demodulated at 2ν using both a sine and cosine phase. The phase of the demodulator references is arbitrary and unknown, but the x axis is assumed to be the East-West axis and the reference arbitrary phase is assumed to be 0° with respect to this coordinate system when time starts. The introduction of a reference phase would not alter the relationship between the non-g-sensitive and g-sensitive portions of the noise.

The race distortion angles, α_1, α_3, β_2 are therefore defined with respect to a coordinate system whose x axis is the axis of zero reference phase.

Demodulating the non-g-sensitive portion of the pickoff signals first,

$$\theta'_x = A_1 \sin(\varphi_1 - \eta) - A_2 \sin\varphi_2 \quad \text{at cos phase} \tag{41}$$

$$= A_1 \cos(\varphi_1 - \eta) - A_2 \cos\varphi_2 \quad \text{at sin phase}$$

$$\theta'_y = -A_1 \cos(\varphi_1 - \eta) - A_2 \cos\varphi_2 \quad \text{at cos phase} \tag{42}$$

$$= A_1 \sin(\varphi_1 - \eta) + A_2 \sin\varphi_2 \quad \text{at sin phase}$$

where

$$A_1 = A\, r_{i_1}\, a$$

$$A_2 = A\, r_{i_3}\, b$$

The angle between the two demodulated vectors θ_x' and θ_y' is found by first finding the angle of each vector in the reference coordinate system followed by finding the tangent of the angle between them. Let

$$\theta_1 = \angle\theta'_x = \tan^{-1} \frac{A_1 \cos x - A_2 \cos\varphi_2}{A_1 \sin x - A_2 \sin\varphi_2}$$

$$\theta_2 = \angle\theta'_y = \tan^{-1} \frac{A_1 \sin x + A_2 \sin\varphi_2}{-A_1 \cos x - A_2 \cos\varphi_2}$$

where $x = \varphi_1 - \eta$

Then

$$\tan(\theta_2 - \theta_1) = \frac{\tan\theta_2 - \tan\theta_1}{1 + \tan\theta_2 \tan\theta_1}$$

$$= \frac{\dfrac{A_1 \sin x + A_2 \sin\varphi_2}{-A_1 \cos x - A_2 \cos\varphi_2} - \dfrac{A_1 \cos x - A_2 \cos\varphi_2}{A_1 \sin x - A_2 \sin\varphi_2}}{1 + \left(\dfrac{A_1 \sin x + A_2 \sin\varphi_2}{-A_1 \cos x - A_2 \cos\varphi_2}\right)\left(\dfrac{A_1 \cos x - A_2 \cos\varphi_2}{A_1 \sin x - A_2 \sin\varphi_2}\right)}$$

After clearing of fractions and combining terms

$$\tan(\theta_2 - \theta_1) = \frac{A_1^2 - A_2^2}{2A_1 A_2 \sin(\varphi_2 - x)}$$

Demodulating the g-sensitive portion of the pickoff signals, we have in the x axis:

$$\theta''_x = \sqrt{2}\,B_2 \left\{ \left[a\left(r_{i_1} \sin(\varphi_1 - \eta) - r_o \sin(\varphi_3 - \eta) \right) - b\, r_{i_3} \sin\varphi_2 \right] \cos\phi + \left[a\left(r_{i_3} \sin(\varphi_2 - \eta) - r_o \cos(\varphi_3 - \eta) \right) - b\, r_{i_1} \sin\varphi_1 \right] \sin\phi \right\} \text{ at cos phase} \tag{43}$$

$$= \sqrt{2}\,B_2 \left\{ \left[a\left(r_{i_1} \cos(\varphi_1 - \eta) - r_o \cos(\varphi_3 - \eta) \right) - b\, r_{i_3} \cos\varphi_2 \right] \cos\phi + \left[a\left(r_{i_3} \cos(\varphi_2 - \eta) + r_o \sin(\varphi_3 - \eta) \right) - b\, r_{i_1} \cos\varphi_1 \right] \sin\phi \right\} \text{ at sin phase} \tag{44}$$

where $r_o = \dfrac{B_1}{\sqrt{2}\,B_2} = \dfrac{K_1}{\sqrt{2}\,K_2}$ and has dimensions of length.

Similarly, in the y axis of the Nutatron we can write

$$\theta''_y = \sqrt{2}\,B_2 \left\{ \left[a\left(-r_{i_1} \cos(\varphi_1 - \eta) + r_o \cos(\varphi_3 - \eta) \right) - b\, r_{i_3} \cos\varphi_2 \right] \cos\phi + \left[a\left(-r_{i_3} \cos(\varphi_2 - \eta) - r_o \sin(\varphi_3 - \eta) \right) - b\, r_{i_1} \cos\varphi_1 \right] \sin\phi \right\} \text{ at cos phase} \tag{45}$$

$$= \sqrt{2}\,B_2 \left\{ \left[a\left(r_{i_1} \sin(\varphi_1 - \eta) - r_o \sin(\varphi_3 - \eta) \right) + b\, r_{i_3} \sin\varphi_2 \right] \cos\phi + \left[a\left(r_{i_3} \sin(\varphi_2 - \eta) - r_o \cos(\varphi_3 - \eta) \right) + b\, r_{i_1} \sin\varphi_1 \right] \sin\phi \right\} \text{ at sin phase} \tag{46}$$

Equations (43), (44), (45), and (46) are parametric equations of ellipses in the x and y axes. The angle variable is θ. Another set of parametric equations in terms of the semi-major and semi-minor axes of an ellipse are

$$\begin{bmatrix} x \\ y \end{bmatrix} = \begin{bmatrix} \cos\gamma & -\sin\gamma \\ \sin\gamma & \cos\gamma \end{bmatrix} \begin{bmatrix} E\cos(\Omega t + \delta) \\ \pm F \sin(\Omega t + \delta) \end{bmatrix} \tag{47}$$

where

x, y	=	x and y axis coordinates in reference system
E	=	semi-major axis of ellipse
F	=	semi-minor axis of ellipse
Ωt	=	$\phi + \pi/4$
γ	=	angle of ellipse semi-major axis with respect to the reference coordinates
δ	=	phase angle of Ωt at points where the semi-major axis intersects the ellipse.

The γ matrix rotates the ellipse coordinates into the reference coordinates.

By manipulating these equations, we can write x and y in terms of the parameter angle, ϕ. The results are

$$\begin{bmatrix} x \\ y \end{bmatrix} = \begin{bmatrix} G_1 \cos(\gamma \pm \epsilon_1) & G_2 \cos(\gamma \pm \epsilon_2) \\ G_1 \sin(\gamma \pm \epsilon_1) & G_2 \sin(\gamma \pm \epsilon_2) \end{bmatrix} \begin{bmatrix} \cos\phi \\ -\sin\phi \end{bmatrix} \tag{48}$$

where

$$G_1 = \left[\frac{E^2 + F^2}{2} - \frac{E^2 - F^2}{2} \sin 2\delta \right]^{1/2}$$

$$G_2 = \left[\frac{E^2 + F^2}{2} + \frac{E^2 - F^2}{2} \sin 2\delta \right]^{1/2}$$

$$\epsilon_1 = \tan^{-1} \left[\frac{F}{E} \tan\left(\frac{\pi}{4} + \delta\right) \right]$$

$$\epsilon_2 = \tan^{-1} \left[\frac{F}{E} \cot\left(\frac{\pi}{4} + \delta\right) \right]$$

The upper signs in equations (47) and (48) represent a coning ellipse, and the lower signs an anti-coning ellipse.

If the angle $\delta \cong 0$, then $\epsilon_1 = \epsilon_2 = \tan^{-1} F/E$ and $G_1 = G_2 = [(E^2+F^2)/2]^{1/2}$. We can now make identifications between equation (48) and equations (43) and (44) in the x axis and between equation (48) and equations (45) and (46) in the y axis for the g-sensitive portion only. Then

$$\begin{aligned}
&\text{(a)} \quad \sqrt{2}\, B_2 \left(a\, r_{i_1} \sin(\varphi_1 - \eta) - a\, r_o \sin(\varphi_3 - \eta) - b\, r_{i_3} \sin\varphi_2 \right) = G_x \cos(\gamma_x \pm \epsilon_x) \\
&\text{(b)} \quad \sqrt{2}\, B_2 \left(a\, r_{i_3} \sin(\varphi_2 - \eta) - a\, r_o \cos(\varphi_3 - \eta) - b\, r_{i_1} \sin\varphi_1 \right) = -G_x \cos(\gamma_x \mp \epsilon_x) \\
&\text{(c)} \quad \sqrt{2}\, B_2 \left(a\, r_{i_1} \cos(\varphi_1 - \eta) - a\, r_o \cos(\varphi_3 - \eta) - b\, r_{i_3} \cos\varphi_2 \right) = G_x \sin(\gamma_x \pm \epsilon_x) \\
&\text{(d)} \quad \sqrt{2}\, B_2 \left(a\, r_{i_3} \cos(\varphi_2 - \eta) + a\, r_o \sin(\varphi_3 - \eta) - b\, r_{i_1} \cos\varphi_1 \right) = -G_x \sin(\gamma_x \mp \epsilon_x) \\
&\text{(e)} \quad \sqrt{2}\, B_2 \left(-a\, r_{i_1} \cos(\varphi_1 - \eta) + a\, r_o \cos(\varphi_3 - \eta) - b\, r_{i_3} \cos\varphi_2 \right) = G_y \cos(\gamma_y \pm \epsilon_y) \\
&\text{(f)} \quad \sqrt{2}\, B_2 \left(-a\, r_{i_3} \cos(\varphi_2 - \eta) - a\, r_o \sin(\varphi_3 - \eta) - b\, r_{i_1} \cos\varphi_1 \right) = -G_y \cos(\gamma_y \mp \epsilon_y) \\
&\text{(g)} \quad \sqrt{2}\, B_2 \left(a\, r_{i_1} \sin(\varphi_1 - \eta) - a\, r_o \sin(\varphi_3 - \eta) + b\, r_{i_3} \sin\varphi_2 \right) = G_y \sin(\gamma_y \pm \epsilon_y) \\
&\text{(h)} \quad \sqrt{2}\, B_2 \left(a\, r_{i_3} \sin(\varphi_2 - \eta) - a\, r_o \cos(\varphi_3 - \eta) + b\, r_{i_1} \sin\varphi_1 \right) = -G_y \sin(\gamma_y \mp \epsilon_y)
\end{aligned} \tag{49}$$

where the subscripts x and y apply to the x or y axis, respectively. The right hand sides of equation (49) are known from plots of experiments. Let these knowns be designated $C_1, C_2, C_3, C_4, C_5, C_6, C_7, C_8$, then the procedure for evaluating the unknowns in these 8 equations is as follows:

Consider the difference of equations (a) and (g) and the sum of equations (c) and (e)

(i) $-2\sqrt{2}\, B_2\, b\, r_{i_3} \sin\varphi_2 = C_1 - C_7$

(j) $-2\sqrt{2}\, B_2\, b\, r_{i_3} \cos\varphi_2 = C_3 + C_5$

Taking the ratio $\frac{(i)}{(j)}$

$$\tan\varphi_2 = \frac{C_1 - C_7}{C_3 + C_5} \tag{50}$$

Similarly, consider equations (b) - (h) and (d) + (f)

(k) $-2\sqrt{2}\, B_2\, b\, r_{i_1} \sin\varphi_1 = C_2 - C_8$

(l) $-2\sqrt{2}\, B_2\, b\, r_{i_1} \cos\varphi_1 = C_4 + C_6$

Then

$$\tan\varphi_1 = \frac{C_2 - C_8}{C_4 + C_6} \tag{51}$$

Further consider equations (a) + (g) and (c) - (e)

(m) $2\sqrt{2}\, B_2\, a\left(r_{i_1} \sin(\varphi_1 - \eta) - r_o \sin(\varphi_3 - \eta)\right) = C_1 + C_7$

(n) $2\sqrt{2}\, B_2\, a\left(r_{i_1} \cos(\varphi_1 - \eta) - r_o \cos(\varphi_3 - \eta)\right) = C_3 - C_5$

and equations (b) + (h) and (d) - (f)

(o) $2\sqrt{2}\, B_2\, a\left(r_{i_3} \sin(\varphi_2 - \eta) - r_o \cos(\varphi_3 - \eta)\right) = C_2 + C_8$

(p) $2\sqrt{2}\, B_2\, a\left(r_{i_3} \cos(\varphi_2 - \eta) + r_o \sin(\varphi_3 - \eta)\right) = C_4 - C_6$

Eliminating r_o terms from these four equations we have after adding equations (m) and (p) and subtracting equations (n) and (o).

(q) $r_{i_1} \sin x + r_{i_3} \cos y = S_1$

(r) $r_{i_1} \cos x - r_{i_3} \sin y = S_2$

where

$$x = \varphi_1 - \eta \qquad S_1 = \frac{(C_1 + C_7 + C_4 - C_6)}{2\sqrt{2}\, B_2\, a}$$

$$y = \varphi_2 - \eta \qquad S_2 = \frac{C_3 - C_5 - C_2 - C_8}{2\sqrt{2}\, B_2\, a}$$

After some algebraic manipulation we can solve equations (q) and (r) simultaneously for x and y in terms of S_1, S_2, r_{i_1} and r_{i_3}. The results are

$$(s) \quad \cos(y + \psi) = \frac{S^2 - r_{i_1}^2 + r_{i_3}^2}{2 S r_{i_3}}$$

$$(t) \quad \sin(x + \psi) = \frac{S^2 + r_{i_1}^2 - r_{i_3}^2}{2 S r_{i_1}}$$

where

$$S = \sqrt{S_1^2 + S_2^2}$$

$$\psi = \tan^{-1} S_2/S_1$$

Let

$$t = S/r_{i_3} \qquad z = y + \psi$$

$$r = \frac{r_{i_1}}{r_{i_3}} \qquad w = x + \psi$$

Then from equations (s) and (t)

$$(u) \quad 2t \cos z = t^2 - r^2 + 1$$

$$(v) \quad 2t \sin w = t^2 + r^2 + 1$$

Solving (u) and (v) simultaneously by eliminating t we have

$$(w) \quad \cos^2 z = 1 - r^2 \cos^2 w$$

Using the trigonometric identity: $\cos^2 z = \frac{1}{2} + \frac{1}{2} \cos 2z$

and letting $w = z + \frac{\lambda}{2}$ we have,

$$\sin(2z - \delta) = \frac{r^2 - 1}{\sqrt{1 + 2 r^2 \cos\lambda + r^4}} \qquad (52)$$

where

$$\delta = \tan^{-1} \frac{1 + r^2 \cos\lambda}{r^2 \sin\lambda}.$$

A knowledge of r and λ allows us to calculate z and w, and knowledge of φ_1 and φ_2 from equations (50) and (51) allows a calculation of η and t.

Finally, rearranging equations (o) and (p), we have

$$(o)\quad r_o \cos(\varphi_3 - \eta) = \frac{-(C_2 + C_8)}{2\sqrt{2}\, B_2\, a} + r_{i_3} \sin y$$

$$(p)\quad r_o \sin(\varphi_3 - \eta) = \frac{C_4 - C_6}{2\sqrt{2}\, B_2\, a} - r_{i_3} \cos y$$

Taking the ratio $\frac{(p)}{(o)}$

$$\tan(\varphi_3 - \eta) = \frac{\dfrac{C_4 - C_6}{2\sqrt{2}\, B_2\, a\, r_{i_3}} - \cos y}{-\dfrac{C_2 + C_8}{2\sqrt{2}\, B_2\, a\, r_{i_3}} + \sin y} \qquad (53)$$

$$(x)\quad t = \frac{S}{r_{i_3}} = \frac{\left[(C_1 + C_7 + C_4 - C_6)^2 + (C_3 - C_5 - C_2 - C_8)^2\right]^{1/2}}{2\sqrt{2}\, B_2\, a\, r_{i_3}}$$

A knowledge of t allows computation of $\varphi_3 - \eta$. Then a knowledge of η provides us with $\varphi_3 = 3\pi/4 - 2\beta_2$ from which β_2 is calculated. Finally $\alpha_1 = \varphi_1 + 2\beta_2$ and $\alpha_3 = \varphi_2 + 2\beta_2/3$ completing the evaluation of the angular constants.

There remains the calculation of distortion magnitudes and spring constants of the bearing. From equation (o)

$$(o)\quad \frac{r_o}{r_{i_3}} = \frac{\dfrac{-(C_2 + C_8)}{2\sqrt{2}\, B_2\, a\, r_{i_3}} + \sin y}{\cos(\varphi_3 - \eta)}$$

where

$$(y)\quad \frac{r_o}{r_{i_3}} = \frac{B_1}{\sqrt{2}\, B_2\, r_{i_3}} = \frac{K_1}{\sqrt{2}\, K_2\, r_{i_3}} \quad \text{and is known}$$

from equation (x)

$$(x)\quad 2\sqrt{2}\, B_2\, a\, r_{i_3} = \frac{c}{t} = \frac{4\sqrt{2}\, \pi\, k_2\, r_{o_2}\, K_2\, W\, a\, r_{i_3}}{R\, K_1^{\,3}}$$

where c and t are known at this point. Substituting (y) in (x)

$$(z)\quad \frac{4\, \pi\, k_2\, r_{o_2}\, K_2\, W\, a\, r_{i_3}}{R\, K_1^{\,2}\, r_o} = \frac{c}{t}$$

Equations (41) and (42) allow us to calculate the constants A_1 and A_2 for the non-g-sensitive noise. Then

$$\text{(aa)} \quad \frac{A_2}{b} = A\, r_{i_3} = \frac{2\pi k_2 r_{O_2} r_{i_3}}{R K_1}$$

Substituting (aa) into (z)

$$\text{(bb)} \quad \frac{2 W a A_2}{b K_1 (r_O/r_{i_3}) r_{i_3}}$$

Solving (bb) for r_{i_3} we have

$$r_{i_3} = \frac{2 W a A_2 t}{b c K_1 (r_O/r_{i_3})} \tag{54}$$

We have a single equation in two unknowns, viz, r_{i_3} and K_1. The value for K_1 can be supplied independently from a bearing analysis. The value for the Nutatron bearing is

$K_1 = 4.63 \times 10^{10}$ dyne/cm.

Now r_{i_3} can be calculated.

Then

$$r_O = \left(\frac{r_O}{r_{i_3}}\right) r_{i_3}$$

$$K_2 = K_1/\sqrt{2}\, r_O \tag{55}$$

$$k_2 r_{O_2} = A_2 R K_1/2\pi b r_{i_3}$$

If $\pi k_2 = K_2$, r_{O_2} can also be estimated.

APPENDIX B: ANALYSIS OF THE CONICAL SPIRAL GROOVE GAS BEARING

The spiral groove bearing was first analyzed by R.T.P. Whipple, and his basic derivation was later applied by Fortescue and Whitley and Williams to obtain circular thrust bearing design data. Briefly, Whipple's derivation assumed an incompressible fluid, negligible inertia effects, and a film thickness that was small compared to other bearing dimensions. He developed his equations for a linear model and assumed that adapting them to a circular thrust bearing would result in negligible error provided the radii were large compared to the width of the bearing area. The boundary conditions, transformed to coordinates along and perpendicular to the grooves, were:

1. Continuity of flux across the groove-ridge boundary:

$$h_1^3 \frac{\partial P_1}{\partial \xi} - h^3 \frac{\partial P}{\partial \xi} = 6\mu U (h_1 - h) \cos\theta \qquad (1)$$

2. Periodicity of the pressure distribution along the direction of motion:

$$a_1 \left(\frac{\partial P_1}{\partial \xi} \cos\theta + \frac{\partial P_1}{\partial \eta} \sin\theta \right) = -a \left(\frac{\partial P}{\partial \xi} \cos\theta + \frac{\partial P}{\partial \eta} \sin\theta \right) \qquad (2)$$

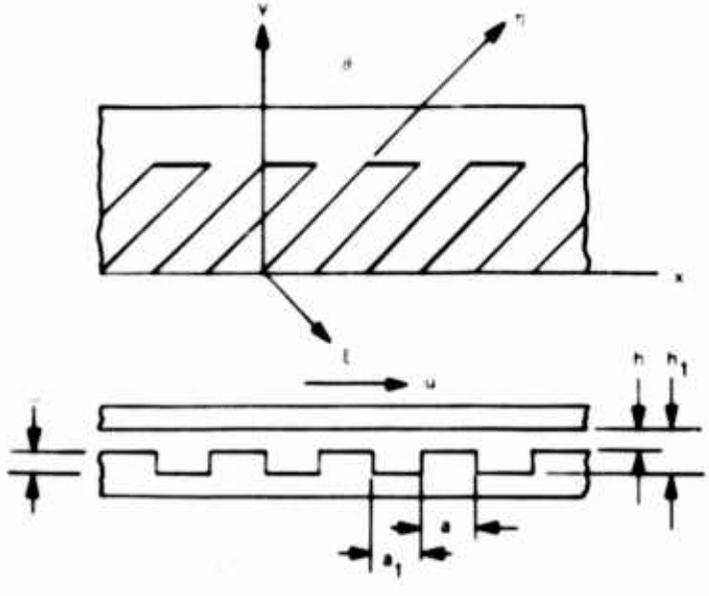

Figure 10. Inclined Groove Bearing Geometry

3. The mean radial flux across the seal belt is equal to the sum of the fluxes in the grooves and ridges:

$$-\frac{1}{(a_1+a)} \frac{\rho}{12\mu} \int_{-a}^{a_1} \frac{h^3 \partial P}{\partial y} dx =$$

$$\frac{1}{(a_1+a)} \frac{\rho}{12\mu} \left[a_1 h_1^3 \left(\frac{\partial P}{\partial \xi} \sin\theta - \frac{\partial P}{\partial \eta} \cos\theta \right) + a h^3 \left(\frac{\partial P}{\partial \xi} \sin\theta - \frac{\partial P}{\partial \eta} \cos\theta \right) \right] \qquad (3)$$

When these equations are solved simultaneously and transformed back to coordinates along and perpendicular to the line of motion, then

$$-h^3 (a_1+a) \left[\frac{\partial P_0}{\partial y} \right]_S + \left[\frac{\partial P_0}{\partial y} \right]_G \left\{ a_1 h_1^3 + a h^3 - \frac{a_1 a \sin^2\theta (h_1^3 - h^3)^2}{a h_1^3 + a_1 h^3} \right\} = 6\mu U \frac{(h_1 - h) a_1 a (h_1^3 - h^3) \sin\theta \cos\theta}{a h_1 + a_1 h^3} \qquad (4)$$

If two bearings are assembled back-to-back so that the pressure of one opposes that of the other, the net flux is zero, and

$$\left[\frac{\partial P_0}{\partial y} \right]_S = 0$$

Furthermore, if $a_1 = a$, this can be written

$$\left[\frac{\partial P_0}{\partial y} \right]_G = \frac{6\mu U (h_1 - h)(h_1^3 - h^3) \sin\theta \cos\theta}{(h_1^3 + h^3)^2 - \sin^2\theta (h_1^3 - h^3)^2} \qquad (5)$$

where $h_1 = h + \Delta$

And since h, h_1 and θ are independent of y, the pressure above ambient at an elemental conical strip is

$$P_o(\theta,h,y) = \frac{6\mu U (h_1-h)(h_1^3-h^3)\sin\theta\cos\theta\, y}{(h_1^3+h^3)^2 - \sin^2\theta\,(h_1^3-h_1^3)^2} \quad (6)$$

The differential normal force acting on an elemental conical surface (Figure A-2) is

$$dF = P_o\, r\, d\phi\, dy \quad (7)$$

Developing this pressure distribution about a conical surface,

$$y = \frac{r_o - r}{\sin\alpha} \quad (8)$$

$$dy = \frac{-dr}{\sin\alpha} \quad (9)$$

$$U = r\omega \quad (10)$$

Therefore,

$$P_o(h,\theta,r) = \frac{6\mu\omega r (r_o-r)(h_1-h)(h_1^3+h^3)\sin\theta\cos\theta}{\sin\alpha\left[(h_1^3+h^3)^2 - \sin^2\theta\,(h_1^3-h^3)^2\right]} \quad (11)$$

The axial force necessary to deflect a pair of conical bearings an axial distance

$$\sigma_a = \delta\sin\alpha$$

$$F_a = \frac{6\mu\omega}{\sin^2\alpha}\int_{r=r_o}^{r=r_1}\int_{\phi=0}^{\phi=2\pi} -r^2(r_o-r)\left[P_o(h-\delta,\theta) - P_o(h+\delta,\theta)\right] d\phi\, dr \quad (12)$$

Integrating, and assuming that $\delta << h$,

$$\frac{F_a}{\sigma_a} = k_a = \frac{6\pi\mu\omega}{h^3}(r_o-r_1)^2(r_o^2+2r_or_1+3r_1^2)J(\gamma,\theta) \quad (13)$$

where $J(\delta,\theta) =$

$$\frac{\sin\theta\cos\theta\gamma^2(2+\gamma)\left[(1+\gamma+\gamma^2)(8+16\gamma+13\gamma^2+5\gamma^3+\gamma^4) - \gamma^2\sin^2\theta\,(3+3\gamma+\gamma^2)^2\right]}{\left[(2+3\gamma+3\gamma^2+\gamma^3)^2 - \gamma^2\sin^2\theta\,(3+3\gamma+\gamma^2)^2\right]^2} \quad (14)$$

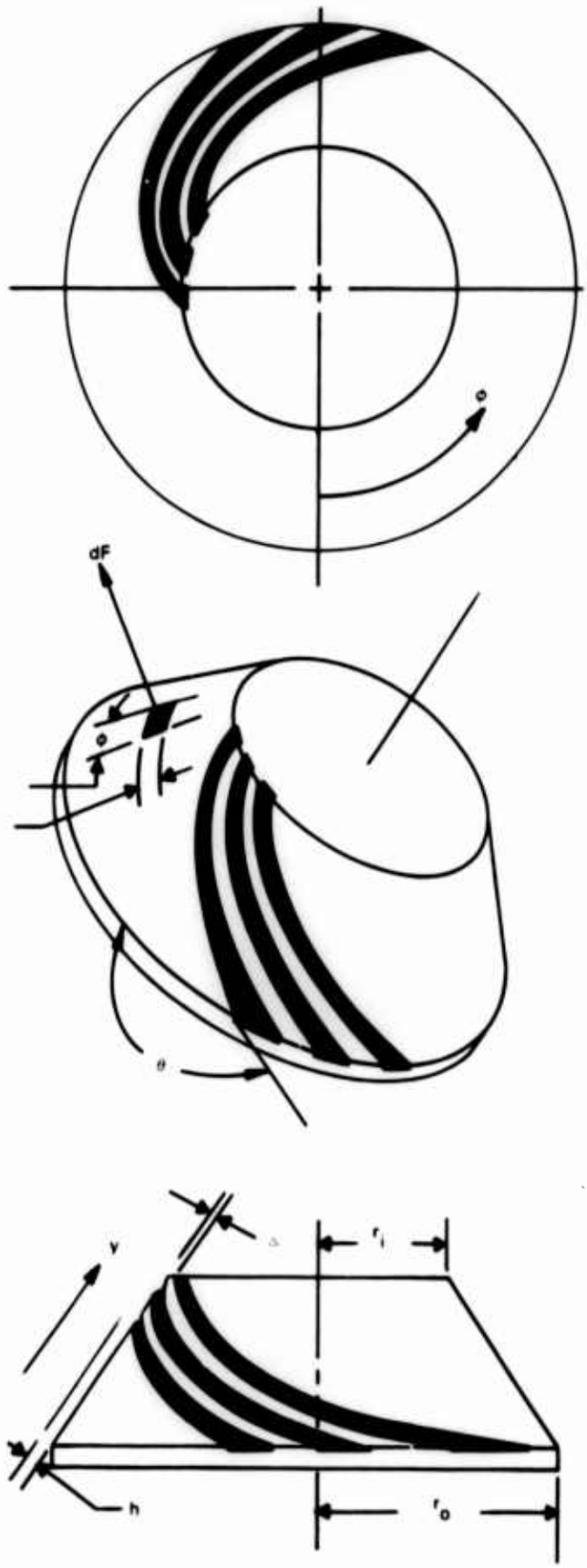

Figure 11. Development of Spiral Grooves on a Conical Surface

A plot of this function is found in Figure A-3. The radial force necessary to deflect a [illegible]nical bearings a radial distance $\sigma_r = \delta \cos \alpha$

$$F_r = \frac{6 \mu \omega}{\sin^2 \alpha} \int_{r = r_0}^{r = r_1} \int_{\phi = 0}^{\phi = 2\pi} -2r^2 (r_0 - r)\, P_0 \left(h \left[1 - \epsilon \cos \phi \right], \theta \right) d\phi\, dr \qquad (15)$$

Integrating, and assuming that $\epsilon << 1$

$$\frac{F_r}{\sigma_a} = k_r = \frac{3\pi \mu \omega \cot^2 \alpha}{h^3} (r_0 - r_i)^2 (r_0^2 + 2 r_0 r_i + 3 r_i^2) J(\gamma, \theta) \qquad (16)$$

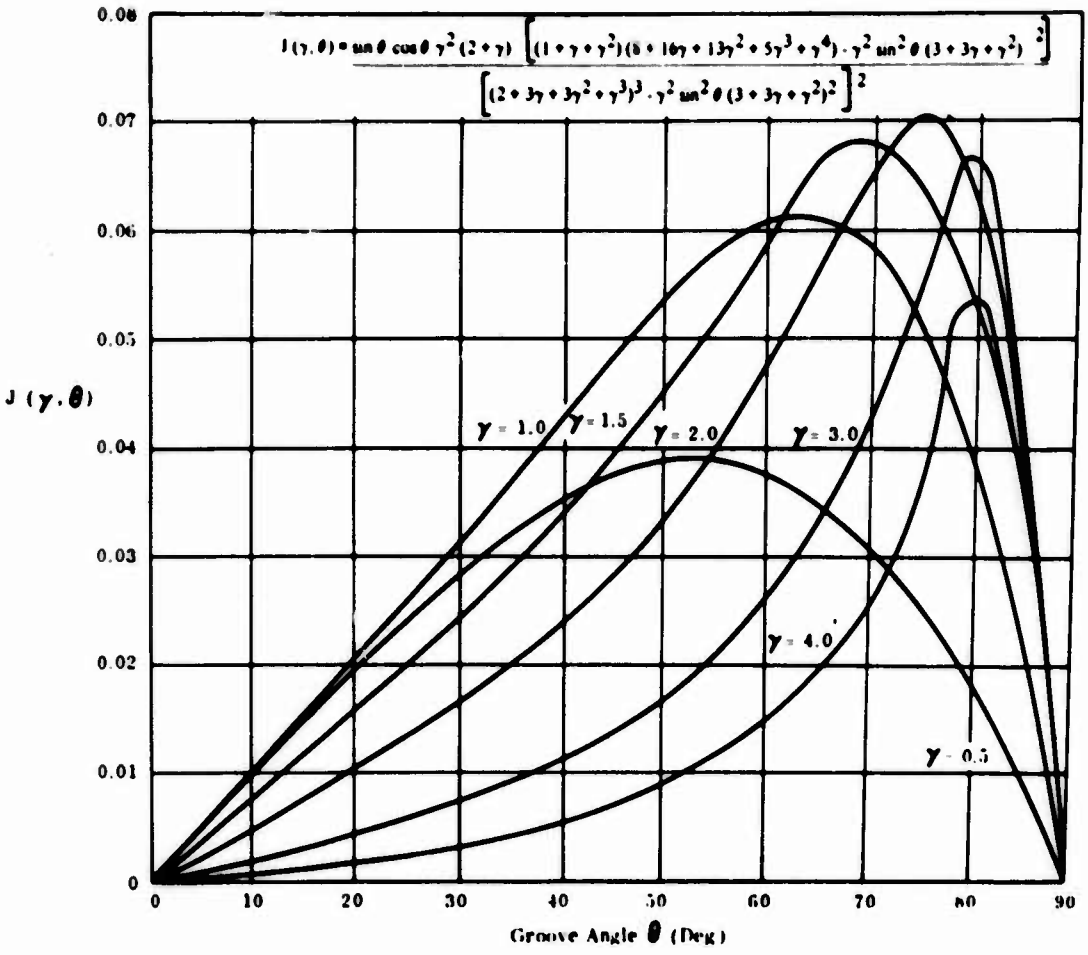

Figure 12. Load Function

References for Section III

1. Harris, Tedric A., Rolling Bearing Analysis, John Wiley & Sons, Inc., 1966.

2. New Departure Division, General Motors Corporation, Analysis of Stresses and Deflections, 1946.

3. Whipple, R.T.P., The Inclined Groove Bearing, United Kingdom Atomic Energy Authority, AERE T/R 622, 1958.

4. Whitley, S. and Williams, L.G., The Gas-Lubricated Spiral Groove Thrust Bearing, United Kingdom Atomic Energy Authority, I.G. Report 28, 1959.

5. Vohr, J.H. and Pan, L.H.T., Design Data Gas-Lubricated Spin-Axis Bearings for Gyroscopes, Mechanical Technology Inc., Report No. MTI-68TR29.

References for Appendix B

1. Whipple, R.T.P. The Inclined Groove Bearing A.E.R.E. T/R 622, Revised U.K.A.E.A. Research Group, Atomic Energy Research Establishment, Harwell, U.K., 1958.

2. Whitley, S. and Williams, L.G. The Gas-lubricated Spiral Groove Thrust Bearing I.G. Report 28 RD/CA U.K.A.E.A. Industrial Group Risley, Warrington, Lancashire U.K., 1959.

3. Fortescue, P. The Derivation of a Generalized Chart for Spiral-Groove Thrust Plate Performance, A.E.R.E.-M804 U.K.A.E.A. Research Group Harwell, U.K., 1960.

4. Whitley, S. The Design of the Spiral Groove Thrust Bearing, Gas Bearing Symposium, University of Southampton, U.K., 1967.

CONFIDENTIAL

DOCUMENT CONTROL DATA - R & D

(Security classification of title, body of abstract and indexing annotation must be entered when the overall report is classified)

1. ORIGINATING ACTIVITY (Corporate author)	2a. REPORT SECURITY CLASSIFICATION
Bell Aerospace Company P.O. Box 1 Buffalo, New York 14240	Confidential
	2b. GROUP IV

3. REPORT TITLE

Nutatron Gyro Development

4. DESCRIPTIVE NOTES (Type of report and inclusive dates)

Final Report April 1, 1969 to September 1, 1970

5. AUTHOR(S) (First name, middle initial, last name)

E. J. Harrison, et al

6. REPORT DATE	7a. TOTAL NO. OF PAGES	7b. NO. OF REFS
January 1971	48	9

8a. CONTRACT OR GRANT NO.	9a. ORIGINATOR'S REPORT NUMBER(S)
F33615-69-C-1722 b. PROJECT NO. 4431 c. d.	Report No. D6006-950004 9b. OTHER REPORT NO(S) (Any other numbers that may be assigned this report) AFAL-TR-70-280

10. DISTRIBUTION STATEMENT

In addition to security requirements which apply to this document and must be met, each transmittal outside the agencies of the U. S. Government must have prior approval of the Air Force Avionics Laboratory.

11. SUPPLEMENTARY NOTES	12. SPONSORING MILITARY ACTIVITY
	AFAL AVNE

13. ABSTRACT

This phase of the Nutatron gyroscopic sensor development was sponsored by the Air Force Avionics Laboratory, WPAFB under Contract F33615-69-C-1722 and by Bell Aerospace Company. The Nutatron gyro features an anisometric rotor which responds to torques by exhibiting minute signals at twice the rotor frequency. These signals are used to automatically compensate for the drift producing torques and as a result the Nutatron is a high performance, low cost gyro with fast reaction time. Under previous contracts, the feasibility of the concept was demonstrated and an engineering model was designed, fabricated, and tested. This report covers a phase of the instrument development which had as its goal the investigation of the effect of bearing imperfections on the instrument performance. During this program unique analyses of bearing noise were made and the results of these analyses show which bearing parameters are important to achieving good Nutatron performance.

DD FORM 1 NOV 68 1473

CONFIDENTIAL

CONFIDENTIAL

14. KEY WORDS	LINK A		LINK B		LINK C	
	ROLE	WT	ROLE	WT	ROLE	WT
gyro						
Nutatron						
ball bearing						
gas bearing						
noise						

CONFIDENTIAL